Original Article

Histological and Immunohistochemical Study of the Effect of Stevia Rebaudiana Extract on the Cerebral Cortex of High Fat Diet-fed Adult Male Albino Rat

Mona Tayssir Sadek[1], Marwa A. A. Ibrahim[1], Doaa A. Radwan[2] and Dina Fouad El Shaer[1]

[1]Department of Histology and Cell Biology, [2]Department of Anatomy, Faculty of Medicine, Tanta University, Egypt

ABSTRACT

Introduction: Obesity is a worldwide health challenge, related to many cognitive and neurodegenerative disorders. The high fat diet (HFD) is considered the main cause of obesity in humans and the standard method for its induction in laboratory animals. Stevia Rebaudiana, a non-caloric natural sweetener, is a promising agent in the management of many medical conditions due to its antioxidant, anti-apoptotic, anti-inflammatory, and hypolipidemic properties.

Aim of the Work: To evaluate the effect of Stevia Rebaudiana extract on the cerebral cortex of high fat diet-fed adult male albino rats.

Materials and Methods: 40 rats were distributed into 4 equal groups; Control group, Stevia-group (daily fed a standard balanced diet & received 400 mg/kg/day of Stevia Rebaudiana extract orally for consecutive 10 weeks), HFD-group (daily fed a HFD for consecutive 10 weeks), and HFD & stevia-group (daily fed a HFD concomitantly with Stevia Rebaudiana extract at similar dose and route as stevia group for consecutive 10 weeks). Specimens of the cerebral cortex were prepared for biochemical, histological, and immunohistochemical techniques.

Results: The HFD-group exhibited a significant increment in (final body weight, weight gain percentage, serum TC, TGs & LDLc, and tissue MDA & MPO), and a significant decrement in (serum HDL and tissue CAT, GPx & SOD). Further, HFD-group exhibited remarkable histological alterations in the cerebral cortex and a significant increment in caspase-3, GFAP, and iNOS immunohistochemical-expression. Co-administration of Stevia Rebaudiana extract with high fat diet prevented most of these biochemical, histological and immunohistochemical alterations.

Conclusion: The obtained results highlighted that Stevia Rebaudiana extract had a potent ameliorative effect versus the induced adverse effects of high fat diet on rats' cerebral cortex.

Received: 09 August 2024 **Accepted:** 16 September 2024

Key Words: Cerebral cortex, GFAP, HFD, iNOS, stevia rebaudiana.

Corresponding Author: Doaa Ahmed Radwan, MD, Department of Anatomy, Faculty of Medicine, Tanta University, Egypt, **Tel.**: +2 011 2078 8201 – +96 6533236020, **E-mail:** dr.doaa.radwan@gmail.com

ISSN: 1110-0559, Vol. 48, No. 3

INTRODUCTION

Globally, obesity has become a serious health issue that endangers millions of people. More than 30% of adults, mainly in developed countries, are suffering from obesity[1]. Unfortunately, numerous health risks and chronic illnesses, including diabetes mellitus, heart and liver diseases, hypertension, metabolic disorders and even certain tumors, are related to obesity[2]. However, it is widely agreed that obesity is preventable by maintaining healthy dietary habits and regular physical activity[3].

High-fat diet (HFD) consumption is a main cause of the increasing prevalence of obesity in humans. Therefore, it has been established as a standard method for obesity induction in laboratory animals in order to study its hazardous effects on different body organs[1,4]. HFD not only elevates serum levels of lipids, triglycerides, ceramides, and cholesterol[5] but also induces serious changes in different brain areas causing regional brain atrophy and decreased neuronal viability in both grey and white matters[6]. Furthermore, it was linked to cognitive impairments, neuroinflammation and apoptosis in certain brain regions[7].

Stevia Rebaudiana (SR) is a plant species from the Asteraceae family. There are several different types of stevia plant preparations that are utilized nowadays, including fresh and dried leaves, leaves' powder as well as extracts and liquid concentrates. Stevia extract, which is 200-300 times sweeter than sugar, is currently used as an excellent substitute for artificial sweeteners[8], as it provides sweetness with low calories and without negative effects on human health[9]. Furthermore, it has been reported that stevia consumption could help in weight regulation without any recognized deleterious effects on the brain tissue[10].

Stevia Rebaudiana was also reported to have anti-hyperglycemic, antioxidant and antihypertensive

DOI: 10.21608/ejh.2024.310649.2120

properties, which make it a plausible additional medical therapy for several diseases[9,11]. Moreover, stevia has gained much interest from the scientific society owing to its beneficial impacts on glucose balance and inflammation which are common obesity-related consequences in addition to, its ability to ameliorate hyperlipidemia and to preserve liver and kidney function indices[12].

Many studies demonstrated the effect of HFD on metabolic conditions and lipid profile in a rat model. However, as far as we know there is no research focusing on the protective role of stevia on the hazards caused by either HFD or obesity on the histological architecture of the cerebral cortex. Thus, the purpose of the current study was to assess the effect of Stevia Rebaudiana extract on the cerebral cortex of adult male albino rats fed a HFD.

MATERIALS AND METHODS

In the current work, 40 adult male albino rats, aged 10 to 13 weeks and weighed 180 to 200 grams each, were used. They were supplied from the animal house of the Histology and Cell Biology Department, Faculty of Medicine, Tanta University, Egypt. The rats were kept in well-ventilated plastic cages under stable environmental conditions (12 hours light /dark-cycle and 22-25°C room temperature). The rats had unrestricted access to standard laboratory diet and water. The safety precautions of the experiment were implemented in compliance with the requirements of the Research Ethics Committee of Tanta Faculty of Medicine, Egypt (Approval-Code NO: 36264PR559/2/24).

Reagents

Pure Stevia Rebaudiana extract powder was purchased from (Steviapura/Stevia group, KÖln-Germany) in the form of highly concentrated stevia extract powder, free of additives (100% pure nature-Item number: 5060050). It was gently extracted from Stevia Rebaudiana plant leaves to produce the herbal stevia extract. It was packaged in resealable tins with tamper-evident closure, each contained 50 g.

Stevia leaves extract was administrated at a daily dosage of 400 mg/kg[13]. In order to prepare the saline solution of stevia leaves extract, each 400 mg of the extract was dissolved in 5 ml saline, so every 1 ml of the resulting solution contained 80 mg of the extract.

Standard and Experimental Diets

The standard balanced diet was designed to provide overall consumed calories (3.5 kcal/g standard diet); 20% from protein, 67% from carbohydrate (5% sucrose & 62% starch,) and 13% from fat. However, the HFD was designed to provide overall consumed calories (4.7 kcal/g HFD diet); 20% from protein, 35% from carbohydrates (7% maltodextrin, 10% starch & 18% sucrose) and 45 % from fat[14].

Experimental Design

After the one-week acclimatization period, the rats were distributed randomly into 4 groups (10 rats for every group):

Group I (Control group): Control rats were equally subdivided into 2 subgroups (5 rats per each):

- Subgroup Ia: Rats in this subgroup were fed a standard balanced diet for 10 consecutive weeks while receiving no treatment.
- Subgroup Ib: Rats in this subgroup were fed a standard balanced diet and were orally administered 1 ml saline daily (the diluting vehicle for Stevia Rebaudiana extract) via gastric gavage for 10 consecutive weeks.

Group II (Stevia group): Rats in this group were fed a standard balanced diet and were orally administered 1 ml/ day of the previously prepared Stevia Rebaudiana extract solution via gastric gavage for 10 consecutive weeks[13].

Group III (HFD-group): Rats in this group were daily fed a HFD for 10 consecutive weeks[15].

Group IV (HFD & stevia-group): Rats in this group were daily fed a HFD and concomitantly received Stevia Rebaudiana extract (at the same dosage and manner as the Stevia group) for 10 consecutive weeks.

Each rat was weighed at the experiment's beginning and end. The percentage of weight gain (%) was determined using the following equation[16].

$$\text{wt gain\%} = \frac{\text{Amount of weight gain in grams}}{\text{Initial weight}} \times 100$$

Blood samples collection

Just after the experimental 10 weeks' period, all rats were fasted for a whole night, and then blood was collected under light ether anesthesia via intra-cardiac puncture, in un-heparinized dry sterile centrifuge bottles[17]. Then immediately under deep ether anesthesia, the sacrification of rats was done via cervical dislocation[18]. The collected blood was allowed to clot at room temperature for ten minutes, then was centrifuged at 3500 rpm / for 10 minutes. Subsequently, the supernatant was cautiously segregated and then preserved at -20°C for assessment of serum levels of total cholesterol (Tc), triglycerides (TGs), low-density lipoprotein cholesterol (LDLc), and high-density lipoprotein cholesterol (HDLc) utilizing commercial kits, following the manufacturer's directions[19].

Cerebral cortex tissue sampling and preparation of tissue homogenates

From each rat, the skull vault was taken off and both cerebral hemispheres were cautiously extracted. Then, the cerebral cortex was dissected and separated out carefully. Each cerebral cortex was then split into two portions; one for the histopathological examination and the other for the preparation of the brain tissue homogenate. The latter was prepared using an ice-cold phosphate-buffered saline (with pH equals 7.4) and a Teflon-glass homogenizer, then it was centrifuged at 5000 rpm for 15 minutes[19]. Later, the

supernatants were segregated and preserved at -20°C to be utilized to detect antioxidant markers, lipid peroxidation and inflammation.

Assessment of antioxidant status, lipid peroxidation and inflammation

The cerebral antioxidant condition was evaluated by measuring catalase activity (CAT), superoxide dismutase (SOD), and glutathione peroxidase (GPx) as described by Chance & Maehly[20], Kakkar *et al*.[21], and Mohandas *et al*.[22] respectively. Furthermore, cerebral cortex malondialdehyde (MDA) level, a lipid peroxidation marker, was measured as formerly illustrated by Ohkawa *et al*.[23], while tissue myeloperoxidase (MPO), an inflammatory index, was assayed as illustrated by Bradley *et al*.[24]. All biochemical techniques were executed in the Biochemistry Department, Faculty of Medicine, Tanta University.

Light microscopic study

The first portion of the cerebral cortex was extracted from all groups, fixed with 10% formalin, dehydrated, cleared, and finally embedded in paraffin to form blocks that were sliced by the microtome at 5 µm-thickness. For the histopathological study, staining the sections with hematoxylin and eosin (H&E) was performed to illustrate the normal histological cerebral cortex characteristics[25].

For immunohistochemical study, caspase-3 immunostaining, for demonstration of the apoptotic cells[26], anti-glial fibrillary acidic protein (GFAP) immunostaining, for illustration of the astrocytes[27], and iNOS immunostaining, for detection of inducible nitric oxide synthase enzyme[28] were performed. Tissue slices were deparaffinized, rehydrated and washed in PBS. Then to reveal the antigens' sites, boiling in sodium citrate buffer (10 mM, pH 6.0) was done for 10-20 minutes. After being allowed to cool for 20 minutes at room temperature, the activity of the endogenous tissue peroxidase was prevented via adding 3% hydrogen peroxide/methanol for 20 minutes, then being washed in PBS. For the next 30 minutes, the sections were kept in 5% human serum albumin (a blocking protein), then washed in PBS for 3 times. The tissue slices were then kept at 4°C over a whole night with the primary antibodies including; rabbit polyclonal anti-caspase-3 antibody (1:500, GB11532, Servicebio, Wuhan, China), rabbit polyclonal anti-GFAP (1:100, RP014, Diagnostic BioSystems Pleasanton, CA, USA), and rabbit polyclonal anti-iNOS antibody (1:200, bs-2072R, Bioss Antibodies Inc., Woburn, Massachusetts, USA). Later, the tissue slices were left for 30 minutes at room temperature with the biotinylated secondary antibody (Vector Labs, Burlingame, California, United States) and subsequently incubated with the streptavidin-peroxidase conjugate for further 30 minutes. 3,3′-diaminobenzidine (DAB) hydrogen peroxide was utilized to detect the immunohistochemical reactivity. All slides were then counterstained with Mayer's hematoxylin. Additionally, for preparation of the negative control, reactions lacking the primary antibodies were done to ensure the specificity of the staining. The positive reactions were brownish cytoplasmic and/or nuclear staining in the neurons for caspase-3, brownish cytoplasmic staining in the astrocytes for GFAP, and brownish studies' cytoplasmic staining in the neurons for iNOS[29]. All light microscopic studies techniques were conducted in the Histology and Cell Biology Department, Faculty of Medicine, Tanta University.

Morphometric study

Images were captured using a digital (Leica ICC50, Switzerland) camera, linked to a light microscope (Leica DM500, Switzerland) in the Histology and Cell Biology Department Faculty of Medicine, Tanta University. For image analysis, "ImageJ" (1.48v NIH, USA) software was utilized. In each slide, 10 random and also non-overlapped fields at a 400x magnification were examined for quantitative measurement of:

1. The apoptotic index (the number of caspase-3 immunopositive cortical neurons x 100 / the total number of cortical neurons) in caspase-3 immunostained sections[30].
2. The mean number of GFAP-positive astrocytes in GFAP immunostained sections[31].
3. The mean area percentage (%) of iNOS positive reaction in the cytoplasm of the neurons in iNOS immunostained sections[14].

Statistical analysis

It was conducted with the Windows IBM SPSS Statistics program (Version 22.0. Armonk, NY: IBM Corp). The one-way analysis of variance (ANOVA) and afterward Tukey's post-hoc test were applied for comparing variations among all studied groups. Results were demonstrated as mean±SD (standard deviation). The differences were regarded as statistically significant if the probability value (p) was lower than 0.05[32].

RESULTS

During the current study, no mortality was reported among the rats of the different groups during the experimental period. Moreover, no remarkable difference was recorded between both subgroups of the control group I (Ia & Ib), as regards the histological, immunohistochemical and biochemical findings. So, in order to simplify the presentation of our results, we referred to them collectively as the control group (I) in the text, tables, histograms and figures. Furthermore, group II (stevia group) revealed similar histological findings and non-statistically significant differences in both biochemical and morphometric data, with respect to the control group.

The body weight (initial, final and percentage (%) of weight gain)

As regards the mean values of the initial body weight of all rats; group II (190.52±6.27), group III (190.04±5.67) and group IV (191.86±7.02) revealed no statistically significant difference (P=0.998, 0.987, 0.99 for groups II, III and IV respectively) versus group I (191±6.44).

However, rats in HFD group III recorded a significant elevation (P<0.05) in their final body weights (287.85±6.62) and in the percentage (%) of weight gain (51.56±4.9) compared to the control group (225.77±3.49, 18.32±4.11 respectively). However, rats in group IV (HFD & stevia-group) displayed a significant reduction (P<0.05) in their final body weights (230.75±5.37) and in the percentage (%) of weight gain (20.4±4.9) with regard to HFD group (III), but it exhibited a non-significant difference (P= 0.13, 0.711 respectively) versus the control group (Table 1, Histogram 1).

Biochemical findings

Serum lipid profile

The lipid profile in HFD group III revealed a significant elevation (P<0.05) in the mean values of TC, TGs and LDLc serum levels (126.66±5.1, 103.85±5.87, 70.36±5.08 respectively) while revealing a significant reduction (P<0.05) in HDLc level (22.01±2.77) compared to the control group (96.15±3.6, 52.48±3.98, 32.4±3.63, 40.3±4.86 for TC, TGs, LDLc and HDLc serum levels respectively).

Inversely, the rats of group IV (HFD & stevia-group) depicted a significant decrement (P<0.05) in serum TC, TGs, and LDLc mean values (100.85±3.31, 57.32±4.76, 36.09±3.5 respectively) and a significant increment (P<0.05) in serum HDLc mean value (38.86±3.77) compared to HFD group III. Meanwhile, these values represented a non-significant difference (P= 0.056, 0.084, 0.156, 0.857 for TC, TGs, LDLc and HDLc serum levels respectively) from group I (Table 2, Histogram 2).

Assessment of antioxidant status, lipid peroxidation and inflammation

As regard the assessment of CAT, GPx and SOD tissue levels, HFD group III recorded a significant decrement (P<0.05) in their mean values (6.6±1.96, 20.71±2.99, 5.41±0.85 respectively) compared to the control group (10.8±2.66, 40.3±2.94, 9.54±0.96 respectively). However, HFD & stevia-group IV recorded a significant increment (P<0.05) in the mean values of CAT (9.6±2.72), GPx (37.49±2.78) and SOD (8.56±0.1) with regard to group III. While a non-significant difference (P= 0.671, 0.14, 0.13 for CAT, GPx and SOD respectively) was detected between group IV and control group (Table 3, Histogram 3).

However, group III revealed a significant elevation (P<0.05) in the mean values of MDA and MPO levels (3.77±0.67, 2.95±0.7 respectively), with regard to the control group (1.6±0.27, 0.85±0.19 respectively), while group IV depicted a significant reduction (P<0.05) in their mean values (2.04±0.34, 1.38±0.29 respectively), compared to group III. Meanwhile, group IV denoted a non-significant difference (P= 0.107) in MDA level and a significant elevation in MPO level versus the control group (Table 3, Histogram 3).

Histological Findings

Hematoxylin and eosin (H&E) stain

Group I and II (Control group and Stevia group): H&E-stained sections of both groups I and II depicted similar findings without remarkable differences. They displayed the normal histological characteristics of the cerebral cortex which was formed of well-organized regularly arranged 6 layers, without sharp limits in between. These layers, from outside inward, were; the molecular layer, the outer granular layer, the outer pyramidal layer, the inner granular layer, the inner pyramidal layer, and finally the polymorphic layer. A regular pia mater was attached to the outer surface of the cerebral cortex without separation (Figure 1-A). The molecular layer contained an enormous amount of fibers and few neuroglial cells, whereas both outer granular and pyramidal layers contained granule cells that displayed rounded cell bodies, open-face nuclei and prominent nucleoli, in addition to small and medium-sized pyramidal cells that appeared triangular with apical dendrites. The surrounding neuropil appeared compact, homogenous and eosinophilic (Figure 1-B). The inner granular layer contained large, rounded granule cells with large open-face nuclei, apparent nucleoli and scant cytoplasm. The inner pyramidal layer contained small rounded glial neurons and large-sized pyramidal cells that revealed rounded vesicular nuclei, apparent nucleoli as well as basophilic cytoplasm. The polymorphic layer contained neurons of various sizes and shapes (Figure 1-C).

Group III (HFD group): The HFD-group exhibited obvious histological alterations compared to the control group, as it showed marked depletion of the cellular elements and loss of the regular lamellar pattern of the cerebral cortex, in addition to neuropil infiltration with small dark glial cells (Figure 2-A). The pia mater appeared discontinued and disrupted with congested blood vessels underneath. The molecular layer showed interstitial hemorrhage, congested blood vessels, vacuolated neuropil, and neuroglial cells with pericellular halos (Figure 2-B). The outer granular layer exhibited lysis in the neuropil and deeply stained granule cells with pericellular halos, while the outer pyramidal layer showed cells with shrunken condensed nuclei. Dilated congested blood vessels lined by vacuolated endothelial cells and red neurons with eosinophilic cytoplasm were also noticed in both outer granular and pyramidal layers (Figure 2-C). Furthermore, the inner granular layer showed congested blood vessels surrounded by a wide perivascular space, and the inner pyramidal layer showed bizarre, deformed, irregularly shaped, darkly stained pyramidal cells surrounded with pericellular halos, in addition to damaged pyramidal cells with karyolitic pale nuclei, and remnants of degenerated pyramidal cells. Additionally, the polymorphic layer exhibited neuroglial cells with darkly stained nuclei and pericellular halos surrounding them. Moreover, the surrounding neuropil appeared vacuolated and lost its normal homogeneity (Figures 2-D,2-E).

Group IV (HFD & stevia-group): H&E-stained sections of HFD & stevia-group exhibited an obvious preservation of most cerebral cortex layers in comparison to group III, and the overlying meninges were intact, regular, and continuous (Figure 3-A). The molecular layer consisted mainly of fibers with relatively few normal glial cells. The outer granular layer contained normal small pyramidal cells and rounded granule cells with open-face nuclei, except for few granule cells that showed darkly stained nuclei with surrounding pericellular haloes. Furthermore, few red neurons exhibiting pyknotic nuclei as well as eosinophilic cytoplasm were observed. The surrounding neuropil was compact and homogenous (Figure 3-B). The outer pyramidal layer exhibited mostly normal medium-sized pyramidal cells, however, few pyramidal cells were dark, shrunken and surrounded by pericellular halos. The inner granular layer contained rounded granule cells displaying open-face nuclei and the neuropil was intact and compact (Figure 3-C). Furthermore, the inner pyramidal layer contained mostly normal large pyramidal cells, but occasionally few shrunken pyramidal cells with dark stained nuclei and pericellular haloes were detected. Few vacuoles were still noticed in the neuropil. The polymorphic layer contained neurons of various sizes and shapes (Figure 3-D).

Immunohistochemical stains

Caspase-3 immunostaining

Both groups I and II showed few neurons, with weak caspase-3-positive nuclear immunoreaction, scattered occasionally in the cerebral cortex layers, except for the outer pyramidal and polymorphic layers, where none could be detected (Figures 4-A,4-B). In group III (HFD group), there were many caspase-3-positive neurons with a strong nuclear immunoreaction in the whole six layers (Figures 4-C,4-D). However, group IV (HFD & stevia-group) depicted few caspase-3-positive neurons with a moderate nuclear immunoreaction dispersed in different layers of the cerebral cortex, except for the inner granular layer and polymorphic layer, where none was detected (Figures 4-E,4-F).

GFAP immunostaining

GFAP immunostained sections in both group I and group II exhibited few dispersed astrocytes with few thin processes, displaying a weak positive cytoplasmic reaction for GFAP, in the six layers of the cerebral cortex (Figures 5-A,5-B). Whereas HFD group showed many astrocytes with numerous thick processes, exhibiting a strong positive cytoplasmic reaction for GFAP, in all cortical layers (Figures 5-C,5-D). Conversely, HFD & stevia group showed some scattered astrocytes with apparent thin processes, displaying a moderate cytoplasmic reaction for GFAP in each of the six layers (Figures 5-E,5-F).

iNOS immunostaining

The iNOS-immunostained sections from group I and group II showed few iNOS-positive neurons with a weak cytoplasmic immunoreaction in the molecular, outer granular, and inner pyramidal layers, while none could be detected in the outer pyramidal, inner granular and polymorphic layers (Figures 6-A,6-B). However, HFD group III showed many neurons with a strongly positive cytoplasmic reaction for iNOS in each of the six cerebral cortex layers (Figures 6-C,6-D). Meanwhile, HFD & stevia group IV exhibited a moderately positive cytoplasmic iNOS immunoreaction in some neurons, mainly in both outer and inner granular layers as well as the inner pyramidal layer, but could not be detected in the molecular, outer pyramidal, or polymorphic layers (Figures 6-E,6-F).

The statistical analysis of the morphometric results

Assessment of the apoptotic index

Regarding the percentage of the apoptotic neurons "the apoptotic index", group III revealed a significant increment(P<0.05) in the apoptotic index (13.13±2.76) compared to the control group (5.51±1.18), while group IV revealed a significant decrement (P<0.05) in the apoptotic index (6.13±1.32) in comparison to group III. Yet, group IV presented non-significant difference (P=0.076) versus the control group I (Table 4,Histogram 4 a).

Assessment of the mean number of GFAP-positive astrocytes

Group III displayed a significant increment (P<0.05) in the mean number of astrocytes with positive reaction for GFAP (48.39±7.85) with regard to the control group (20.5±4.2). Whereas, group IV displayed a significant decrement (P<0.05) in GFAP positive astrocytes' mean number (22.48±4.28) with respect to group III. Meanwhile, a non-significant statistical difference (P=0.052) was detected between group IV and group I (Table 4, Histogram 4 b).

Assessment of the mean area percentage (%) of iNOS

As regards the mean iNOS area percentage, there was a significant increment (P<0.05) in group III (16.46±2.91) with respect to the control group (3.71±0.68), while in group IV there was a significant decrement (P<0.05) in iNOS area % (4.29±1.33) in comparison with group III. Moreover, group IV represented a non-significant difference in iNOS mean area % versus the control group (Table 4, Histogram 4c).

DISCUSSION

Obesity is a serious worldwide health problem, related to both cognitive and neurodegenerative disorders. High fat diet intake is a common animal model, used to study obesity, insulin resistance and metabolic diseases[33,34]. So, in the current work, the HFD was used as a method to induce obesity in rats in order to assess its effect on

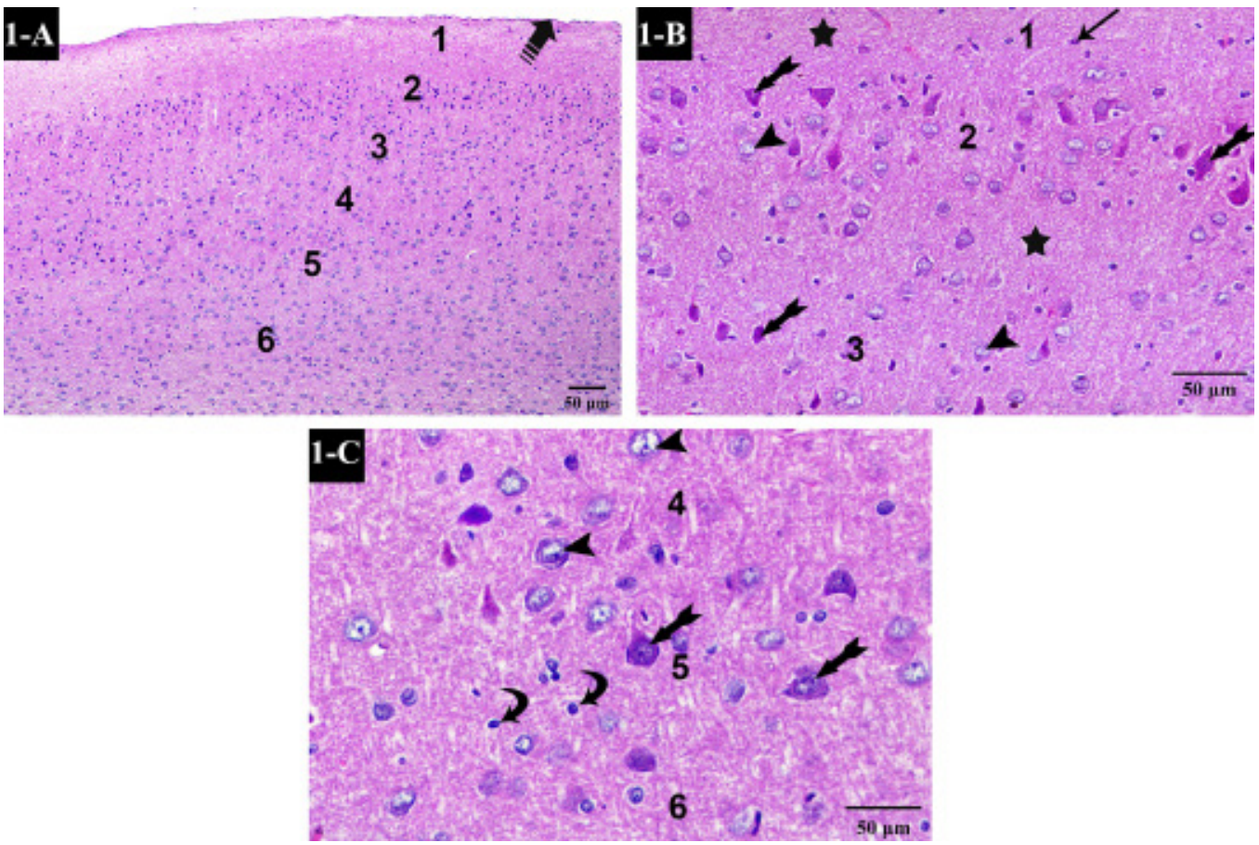

Fig. 1: H&E-stained sections from the control group show [A] Normal cerebral cortex displaying well organized regularly arranged six layers; molecular layer (1), outer granular layer (2), outer pyramidal layer (3), inner granular layer (4), inner pyramidal layer (5), and polymorphic layer (6). Notice intact regular pia mater (striped arrow); [B] The molecular layer (1) with normal few neuroglial cells (thin arrow), the outer granular layer (2) and the outer pyramidal layer (3) with normal rounded granule cells having open-face nuclei (arrowheads) and small & medium-sized pyramidal cells appearing triangular in shape with apical dendrites (bifid arrows); [C] The inner granular layer (4) contains large rounded granule cells displaying open-face nuclei and prominent nucleoli, as well as scanty cytoplasm (arrowheads). The inner pyramidal layer (5) contains large-sized pyramidal cells displaying rounded vesicular nuclei, apparent nucleoli, as well as basophilic cytoplasm (bifid arrows), and small rounded glial neurons (curved arrows). The polymorphic layer (6) contains neurons of various sizes and shapes (H&E A×100 - B, C ×400, scale bar= 50 µm).

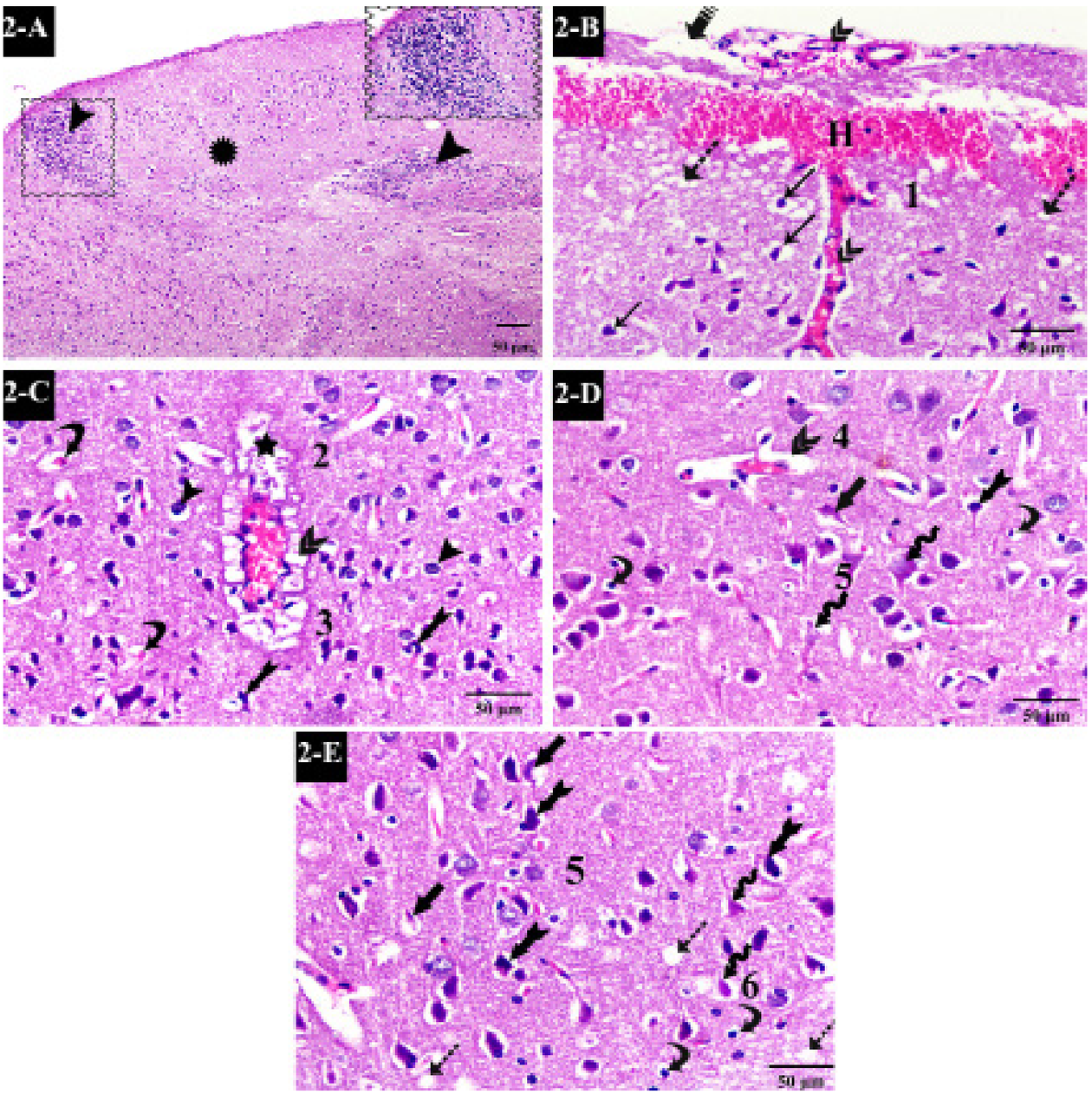

Fig. 2: H&E-stained sections from the HFD group show [A] Marked depletion of the cellular elements and loss of the regular lamellar appearance of the cerebral cortex (asterisk) and infiltration with small dark glial cells (arrowheads); [B] Discontinued pia mater (striped arrow), interstitial hemorrhage (H), vacuolated neuropil (dotted arrows), and neuroglial cells surrounded by pericellular halos (thin arrows) in the molecular layer (1). Notice dilated congested blood vessels (double arrows); [C] The outer granular layer (2) exhibits lysis in the neuropil (star) and deeply stained granule cells with pericellular halos (arrowheads). The outer pyramidal layer (3) shows neurons with shrunken condensed nuclei (bifid arrows). A dilated congested blood vessel lined by vacuolated endothelial cells (double arrows) and red neurons with eosinophilic cytoplasm (curved arrows) are seen in both layers (2&3); [D] The inner granular layer (4) contains a congested blood vessel surrounded by wide perivascular space (double arrows). The inner pyramidal layer (5) shows a bizarre-shaped pyramidal cell (thick arrow), a darkly stained pyramidal cell surrounded by haloes (bifid arrow), and some degenerated pyramidal cells with pale karyolitic nuclei (wavy arrows). Notice pericellular halos around the neuroglial cells (curved arrows); [E] The inner pyramidal layer (5) contains irregular deformed pyramidal cells with darkly stained nuclei and pericellular haloes (bifid arrows), remnants of damaged pyramidal cells (thick arrows) and some pyramidal cells with pale karyolitic nuclei (wavy arrows). The polymorphic layer (6) shows neuroglial cells with darkly stained nuclei and pericellular halos surrounding them (curved arrows). Notice the surrounding neuropil appears vacuolated in the inner pyramidal (5) and the polymorphic (6) layers (dotted arrows). (H&E A×100; inset x400 - B, C, D, E ×400, scale bar= 50 µm).

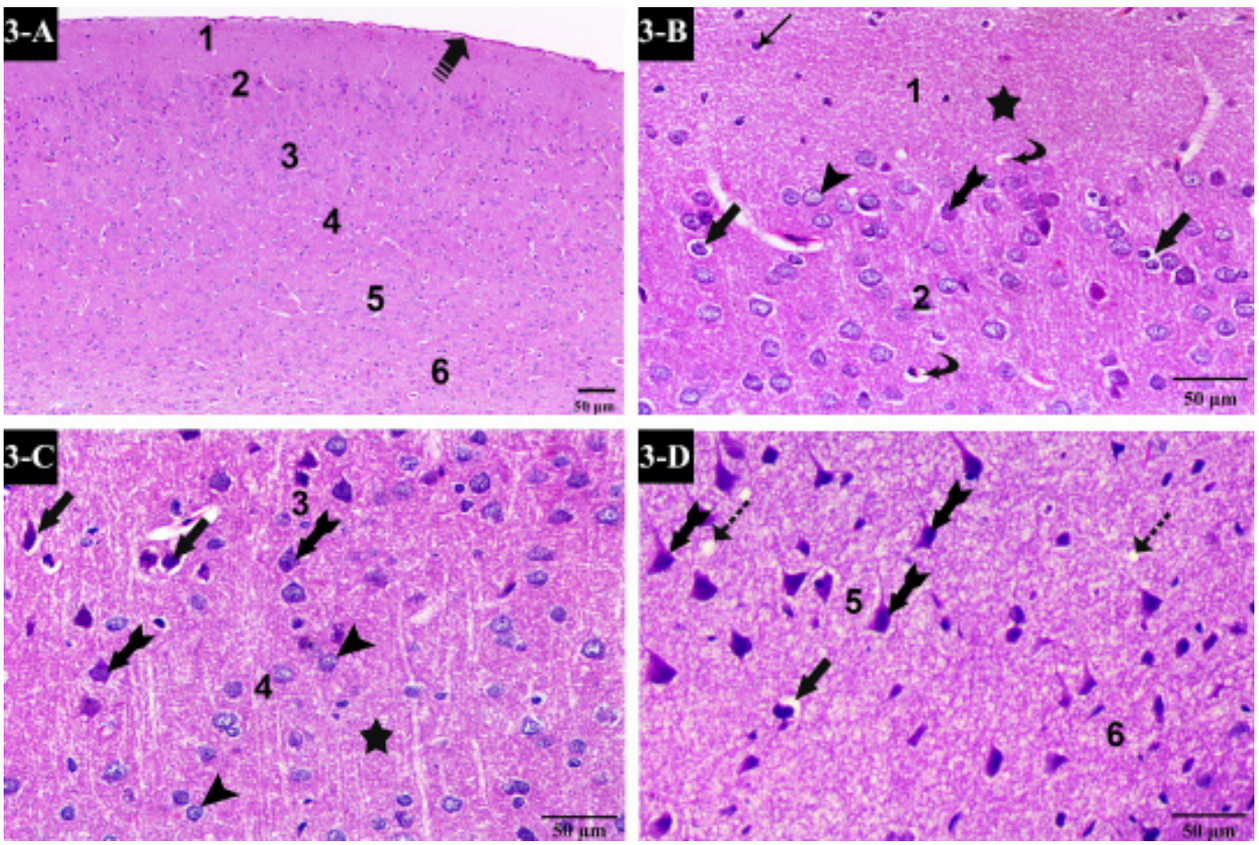

Fig. 3: H&E-stained sections from the HFD & stevia-group show [A] The cerebral cortex with its well-arranged six layers; molecular layer (1), outer granular layer (2), outer pyramidal layer (3), inner granular layer (4), inner pyramidal layer (5), and polymorphic layer (6). Notice intact regular pia mater (stripped arrow); [B] An intact molecular layer (1) with normal glial cells (thin arrow). The outer granular layer (2) shows normal small pyramidal cells (bifid arrow) and rounded granule cells with open-face nuclei (arrowhead) except for few granule cells that have dark nuclei and pericellular haloes (thick arrows). Few red neurons display pyknotic nuclei and eosinophilic cytoplasm (curved arrows). Notice the compact neuropil (star); [C] Mostly normal medium-sized pyramidal cells (bifid arrows) in the outer pyramidal layer (3). Few pyramidal cells appear dark, shrunken, and surrounded by pericellular halos (thick arrows). The inner granular layer (4) contains normal granule cells appearing rounded with open-face nuclei (arrowheads). Notice the compact neuropil (star); [D] The inner pyramidal layer (5) contains mostly normal large-sized pyramidal cells (bifid arrows). A pyramidal cell appears shrunken with deeply stained nuclei surrounded by a pericellular halo (thick arrow). The polymorphic layer (6) contains neurons of various sizes and shapes. Notice few vacuoles in the neuropil (dotted arrows) (H&E A×100 - B, C, D, ×400, scale bar= 50 µm).

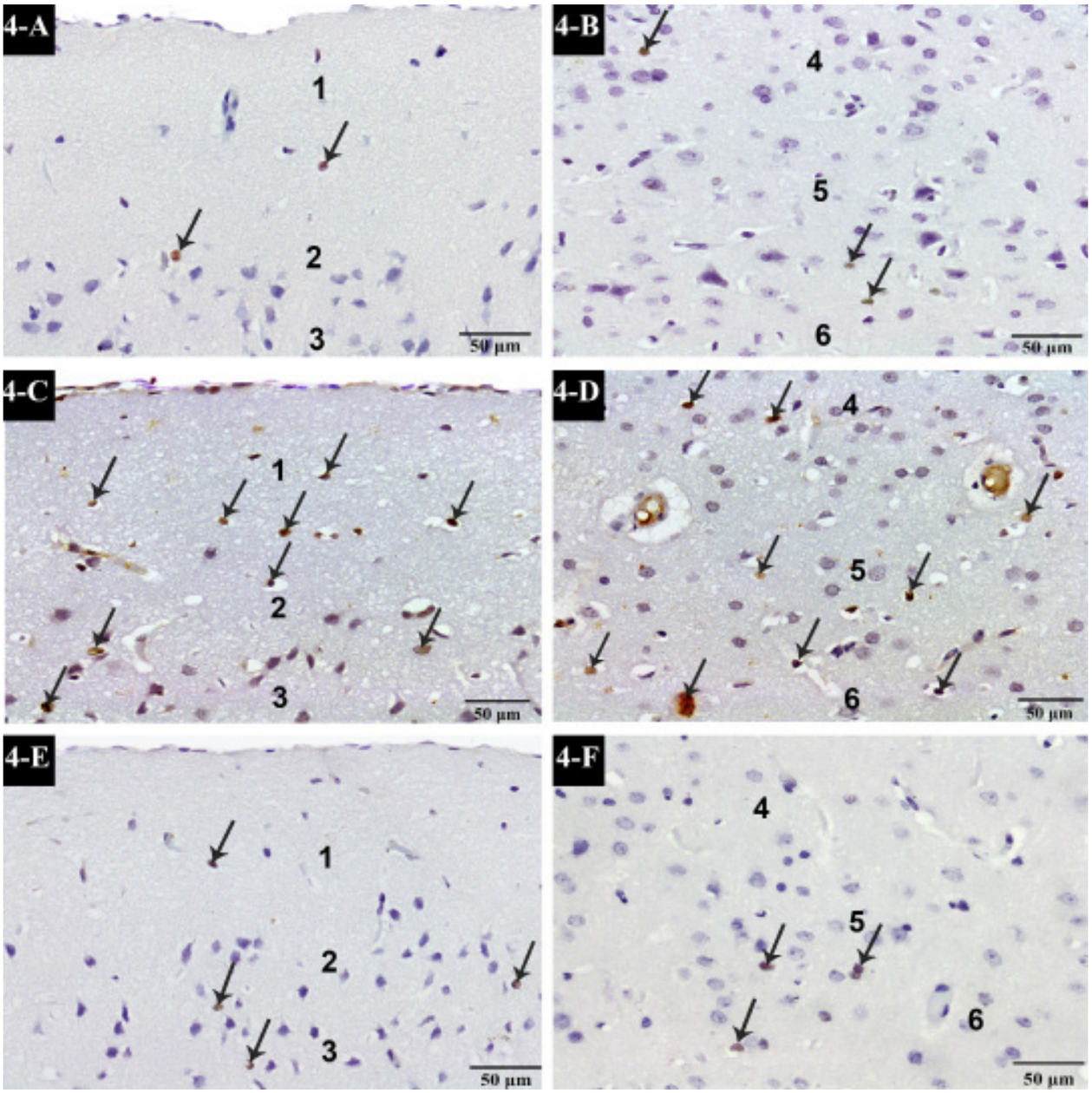

Fig. 4: Caspase-3-immunostained sections from all studied groups. The control group shows [A] Few caspase-3 +ve neurons with a weak nuclear reaction (arrows) in the molecular (1) and the outer granular (2) layers, while none can be detected in the outer pyramidal layer (3); [B] Few caspase-3 +ve neurons with a weak nuclear reaction (arrows) in both inner granular (4) and pyramidal layers (5), whereas none can be detected in the polymorphic layer (6). The HFD group shows [C] Many caspase-3 +ve neurons with a strong nuclear reaction (arrows) in the molecular layer (1), the outer granular layer (2), and the outer pyramidal layer (3); [D] Many caspase-3 +ve neurons with a strong nuclear reaction (arrows) in the inner granular (4), the inner pyramidal (5), and the polymorphic (6) layers. The HFD & stevia-group shows [E] Few caspase-3 +ve neurons with a moderate nuclear reaction (arrows) in the molecular (1), the outer granular (2), and the outer pyramidal (3) layers; [F] Few caspase-3 +ve neurons with a moderate nuclear immunoreaction (arrows) mainly in the inner pyramidal layer (5) and none can be detected in the inner granular (4) and the polymorphic (6) layers. (Caspase-3 × 400, scale bar= 50 µm).

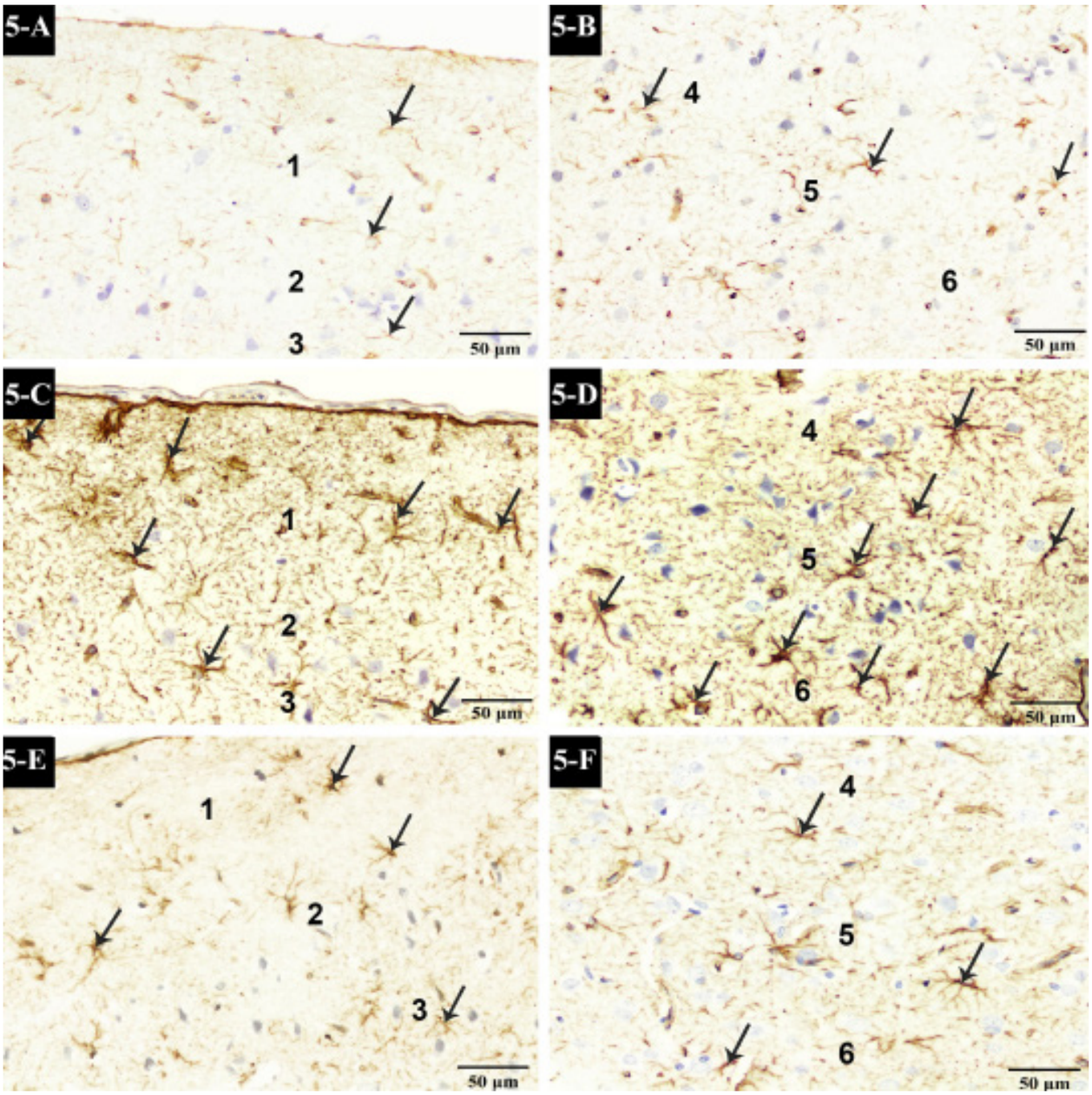

Fig. 5: GFAP-immunostained sections from all studied groups. The control group shows [A] Few dispersed GFAP +ve astrocytes with few thin processes and a weak cytoplasmic reaction (arrows) in the molecular (1), the outer granular (2), and the outer pyramidal (3) layers; [B] Few dispersed GFAP +ve astrocytes with few thin processes and a weak cytoplasmic reaction (arrows) in the inner granular (4), the inner pyramidal (5), and the polymorphic (6) layers. The HFD group shows [C] Numerous GFAP +ve astrocytes with abundant thick processes and a strong cytoplasmic reaction (arrows) in the molecular (1), the outer granular (2), and the outer pyramidal (3) layers; [D] Numerous GFAP +ve astrocytes with multiple thick processes and a strong cytoplasmic reaction (arrows) in the inner granular (4), the inner pyramidal (5), and the polymorphic (6) layers. The HFD & stevia-group shows [E] Some scattered GFAP +ve astrocytes with apparent thin processes and a moderate cytoplasmic reaction in the molecular (1), the outer granular (2), and the outer pyramidal (3) layers; [F] Some scattered GFAP +ve astrocytes with apparent thin processes and a moderate cytoplasmic reaction in the inner granular (4), the inner pyramidal (5), and the polymorphic (6) layers. (GFAP ×400, scale bar= 50 µm).

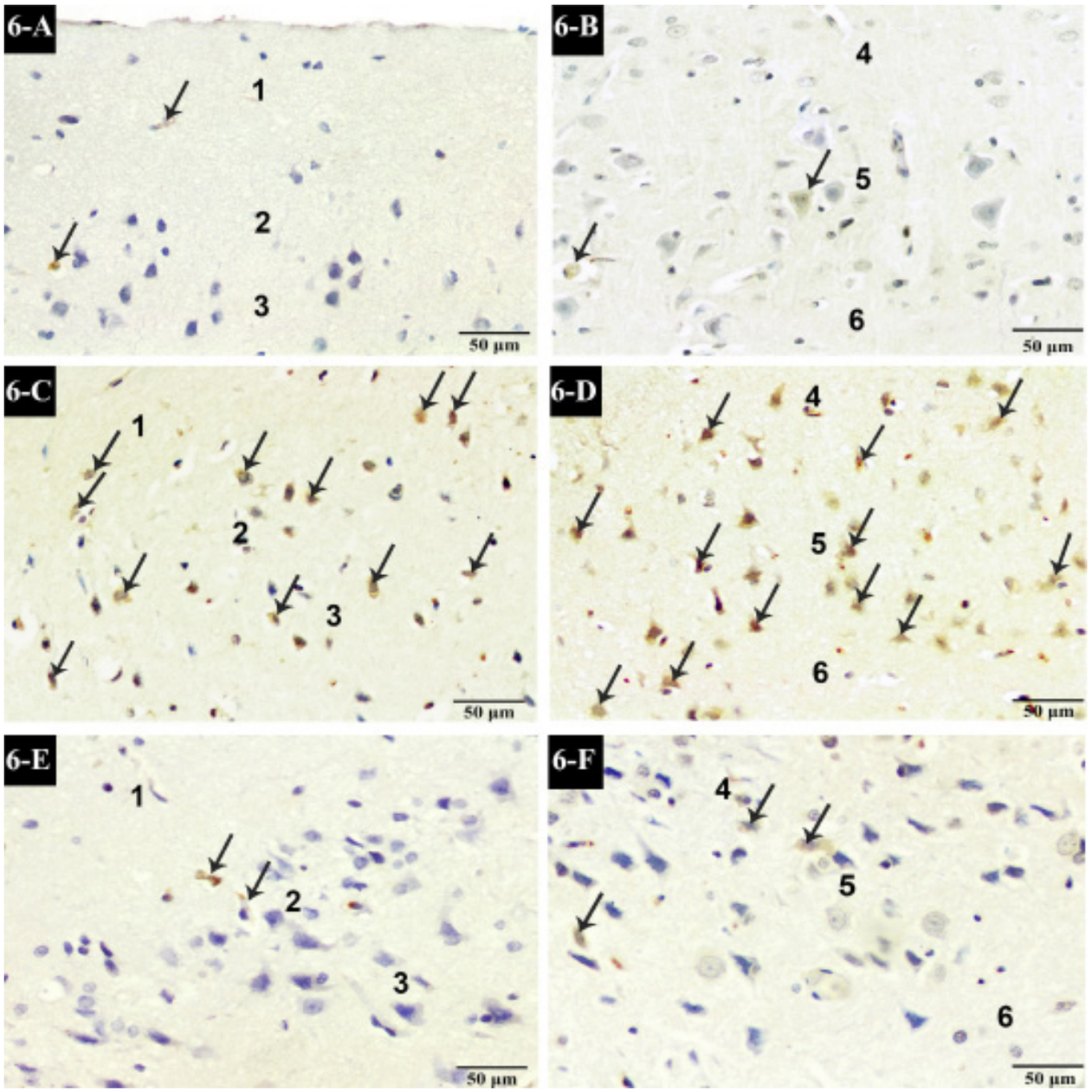

Fig. 6: iNOS-immunostained sections from all studied groups. The control group shows [A] Few iNOS +ve nerve cells displaying a weak cytoplasmic reaction (arrows) in the molecular (1) and the outer granular (2) layers, while none can be detected in the outer pyramidal layer (3); [B] Few iNOS +ve cells with a weak cytoplasmic reaction (arrows) in the inner pyramidal layer (5), while none can be detected in the inner granular (4) or the polymorphic (6) layers. The HFD group shows [C] Many iNOS +ve cells with a strong cytoplasmic reaction (arrows) in the molecular (1), the outer granular (2) and the outer pyramidal (3) layers; [D] Many iNOS +ve cells with a strong cytoplasmic reaction (arrows) in both inner granular (4) and pyramidal (5) layers as well as the polymorphic layer (6). The HFD & stevia-group shows [E] Some iNOS +ve cells with a moderate cytoplasmic reaction (arrows) in the outer granular layer (2), while none can be detected in the molecular layer (1) or the outer pyramidal layer (3); [F] Some iNOS +ve cells with a moderate cytoplasmic immunoreaction (arrows) in both inner granular (4) and pyramidal (5) layers but cannot be detected in the polymorphic layer (6). (iNOS ×400, scale bar= 50 µm).

Table 1: Statistical analysis of the mean values of the initial body weight (g), final body weight (g) and the percentage of weight gain (%) of rats in all studied groups.

Groups Parameters	Group I (Control group) (n = 10)	Group II (Stevia group) (n = 10)	Group III (HFD-group) (n = 10)	Group IV (HFD & Stevia-group) (n = 10)
	Mean ± SD			
Initial body weight (g)	191±6.44	190.52±6.27	190.04±5.67	191.86±7.02
Final body weight (g)	225.77±3.49	221.95±3.65	287.85±6.62[a, b]	230.75±5.37[c]
Percentage of weight gain (%)	18.32±4.11	16.42±3.08	51.56±4.9[a, b]	20.4±4.9[c]

Data are shown as Mean ± Standard deviation (SD), one-way ANOVA followed by Tukey's post-hoc test was used. Statistical significance was set at *p value*<0.05, significance is indicated by the superscript letters [a, b, c] against groups I, II and III respectively (n = number of rats, g = grams).

Table 2: Statistical analysis of the mean values of TC, TGs, LDLc and HDLc serum levels of the rats in all studied groups.

Groups Parameters	Group I (Control group) (n = 10)	Group II (Stevia group) (n = 10)	Group III (HFD-group) (n = 10)	Group IV (HFD & Stevia-group) (n = 10)
	Mean ± SD			
TC (mg/dL)	96.15±3.6	94.66±3.62	126.66±5.1[a,b]	100.85±3.31[c]
TGs (mg/dL)	52.48±3.98	51.37±2.12	103.85±5.87[a,b]	57.32±4.76[c]
LDLc (mg/dL)	32.4±3.63	32.03±2.73	70.36±5.08[a,b]	36.09±3.5[c]
HDLc (mg/dL)	40.3±4.86	39.89±4.5	22.01±2.77[a,b]	38.86±3.77[c]

Data are shown as Mean ± Standard deviation (SD), one-way ANOVA followed by Tukey's post-hoc test was used. Statistical significance was set at *p value*<0.05, significance is indicated by the superscript letters [a, b, c] against groups I, II and III respectively. (TC: total cholesterol, TGs: triglycerides, LDLc: low-density lipoprotein cholesterol, HDLc: high-density lipoprotein cholesterol, n = number of rats, mg/dL: milligrams per decilitre).

Table 3: Statistical analysis of the mean values of CAT, GPx, SOD, MDA and MPO levels in the cerebral cortex homogenates of the rats in all studied groups.

Groups Parameters	Group I (Control group) (n = 10)	Group II (Stevia group) (n = 10)	Group III (HFD-group) (n = 10)	Group IV (HFD & Stevia-group) (n = 10)
	Mean ± SD			
CAT (umol/min./mg protein)	10.8±2.66	11.1±2.02	6.6±1.96[a,b]	9.6±2.72[c]
GPx (nmol/mg protein)	40.3±2.94	40.63±2.65	20.71±2.99[a,b]	37.49±2.78[c]
SOD (U/mg protein)	9.54±0.96	10.1±1.07	5.41±0.85[a,b]	8.56±0.1[c]
MDA (nmol/mg protein)	1.6±0.27	1.63±0.25	3.77±0.67[a,b]	2.04±0.34[c]
MPO (µmol/min./mg protein)	0.85±0.19	0.92±0.19	2.95±0.7[a,b]	1.38±0.29[a,c]

Data are shown as Mean ± Standard deviation (SD), one-way ANOVA followed by Tukey's post-hoc test was used. Statistical significance was set at *p value*<0.05, significance is indicated by the superscript letters [a, b, c] against groups I, II and III respectively. (CAT:catalase activity, GPx: glutathione peroxidase, SOD: superoxide dismutase, MDA: malondialdehyde, MPO: myeloperoxidase, n = number of rats, g =grams).

Table 4: Statistical analysis of the apoptotic index, the mean number of GFAP-positive astrocytes and the area % of iNOS in all studied groups.

Groups Parameters	Group I (Control group) (n = 10)	Group II (Stevia group) (n = 10)	Group III (HFD-group) (n = 10)	Group IV (HFD & Stevia-group) (n = 10)
	Mean ± SD			
The Apoptotic Index	5.51±1.18	5.46±1.3	13.13±2.76[a,b]	6.13±1.32[c]
The Mean Number of GFAP-positive Astrocytes	20.5±4.2	19.96±4.62	48.39±7.85[a,b]	22.48±4.28[c]
Area % of iNOS	3.71±0.68	3.6±0.72	16.46±2.91[a,b]	4.29±1.33[c]

Data are shown as Mean ± standard deviation (SD), one-way ANOVA followed by Tukey's post-hoc test was used. Statistical significance was set at *p value*<0.05, significance is indicated by the superscript letters [a, b, c] against groups I, II and III respectively. (iNOs: inducible nitric oxide synthase, GFAP: glial fibrillary activating protein, n= number of rats).

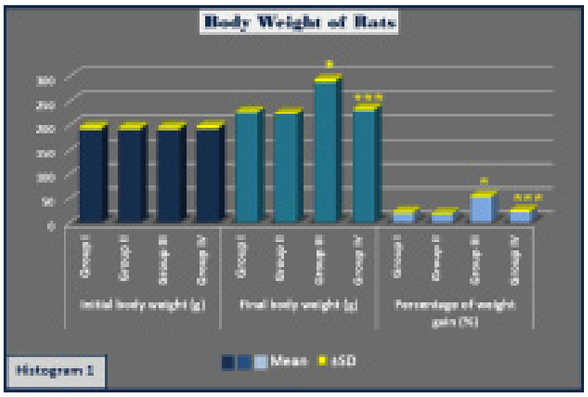

Histogram 1: Statistical analysis of the mean values of the initial body weight (g), final body weight (g), and the percentage of weight gain (%) in all studied groups. (g = grams, *: significant vs group I, ***: significant vs group III).

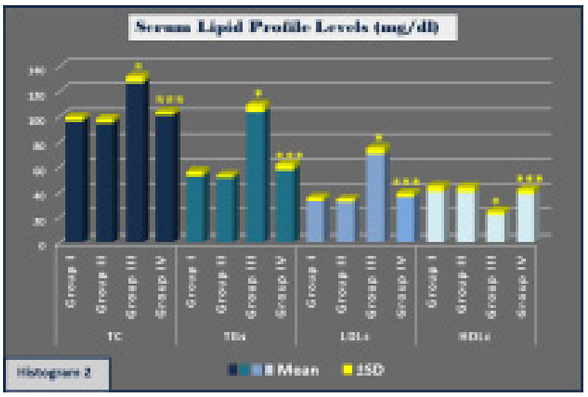

Histogram 2: Statistical analysis of the mean values of TC, TGs, LDLc and HDLc serum levels in all studied groups. (TC: total cholesterol, TGs: triglycerides, LDLc: Low-density lipoprotein cholesterol, HDLc: high-density lipoprotein cholesterol, *: significant vs group I, ***: significant vs group III).

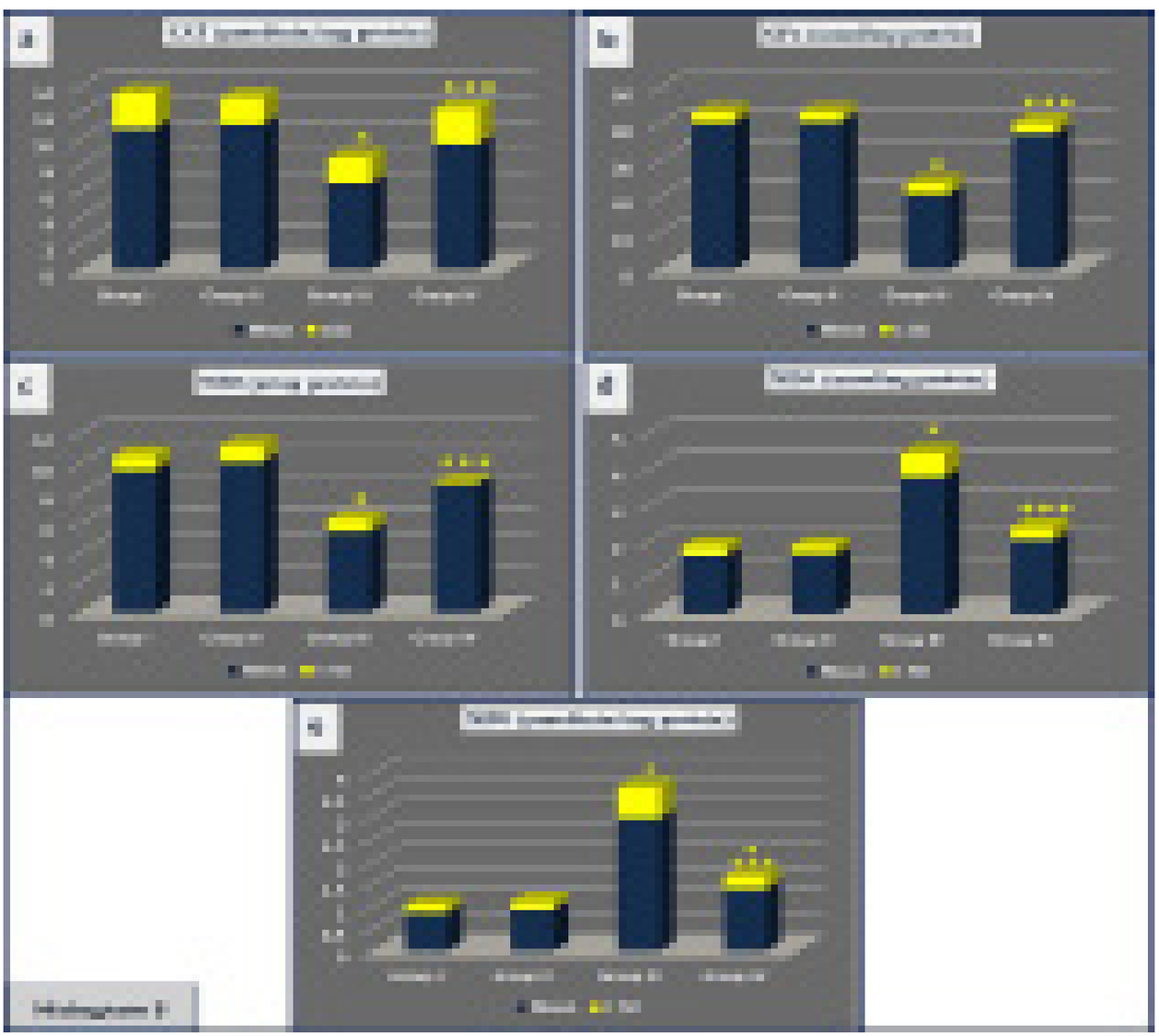

Histogram 3: Statistical analysis of the mean values of (a) CAT, (b) GPx, (c) SOD, (d) MDA and (e) MPO. (CAT: catalase activity, GPx: glutathione peroxidase, SOD: superoxide dismutase, MDA: malondialdehyde, MPO: myeloperoxidase, *: significant vs group I, ***: significant vs group III).

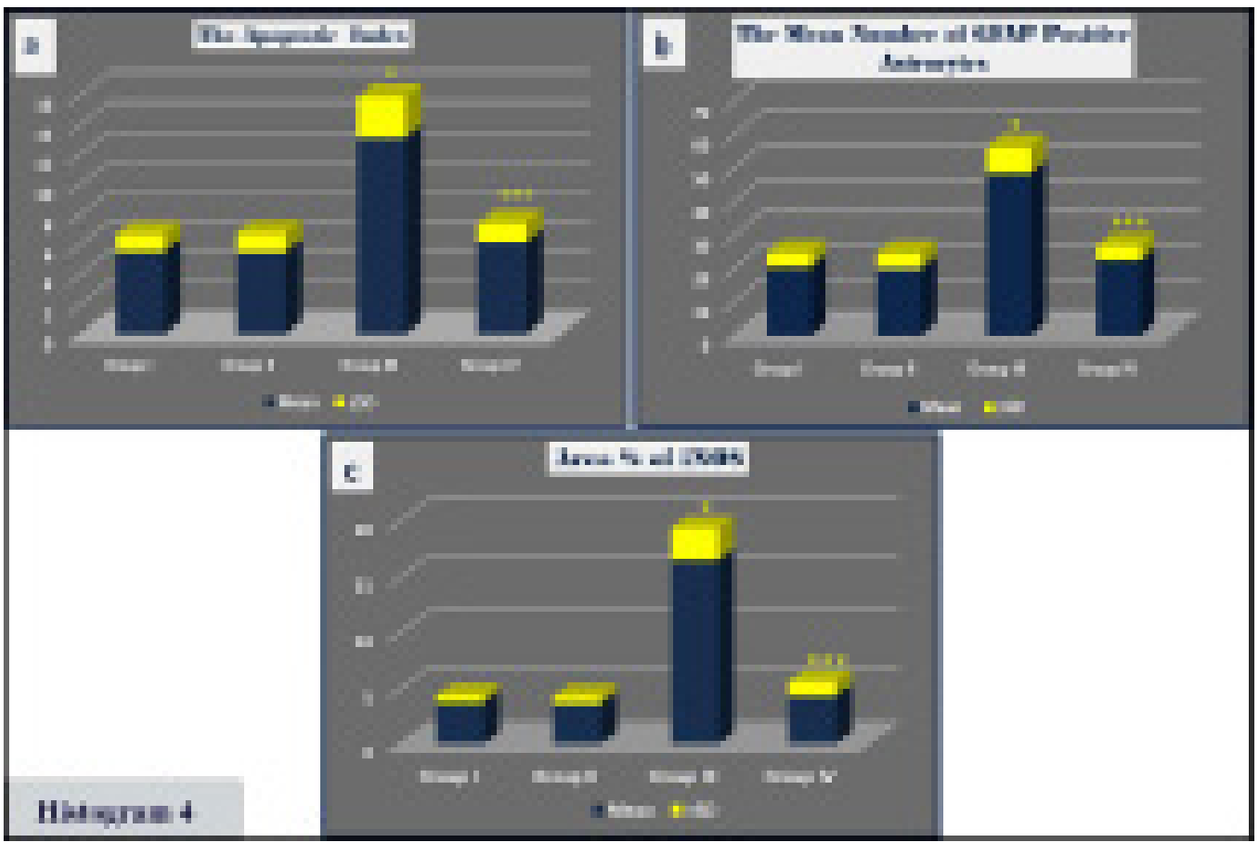

Histogram 4: Statistical analysis of (a) the apoptotic index, (b) the mean number of GFAP-positive astrocytes, and (c) the area % of iNOS in all studied groups. (iNOs: inducible nitric oxide synthase, GFAP: glial fibrillary activating protein, *: significant vs group I, ***: significant vs group III).

the histological architecture of the cerebral cortex and to evaluate the possible ameliorative role of Stevia Rebaudiana extract on this effect.

In this work, the rats of HFD group III displayed a significant increment in their total body weight and weight gain percentage versus the control group I. Similar results were recorded by Alkan *et al*.[35] and Suleiman *et al*.[36]. They attributed the weight gain to increased appetite, food intake and fat deposition in the adipocytes secondary to decreased expression of the brain-derived neurotrophic factor (BDNF), that controls food intake as well as energy metabolism, insulin sensitivity, neuronal growth and survival in addition to, synaptic plasticity.

The lipid profile of rats in HFD group III revealed significantly elevated serum TC, TGs, LDLc levels and a significantly decreased serum HDLc level, with respect to the control group. This agreed with Suleiman *et al*.[36] and Yousef[37]. HFD was reported to increase chylomicrons production in the intestine, that are transformed in the blood into free fatty acids. Later, the fatty acids enter the liver where they are transformed into triglycerides then VLDL and finally LDL[38].

Moreover, HFD group III depicted a significant decrement in the tissue levels of the cerebral oxidative stress markers (CAT, SOD, GPx) together with a significant increment in lipid peroxidation marker (MDA) and inflammatory marker (MPO) levels. Similar results were recorded in the hepatic, cardiac and renal tissues[39], in the cerebral cortical tissue[14,40] and in the testes[36] of HFD-fed rats.

HFD, hyperlipidemia and obesity were all implicated in inducing oxidative stress and inflammatory condition in the nervous system especially the cerebral cortex via variable mechanisms[33,38]. One mechanism involves increased fatty acid oxidation in the mitochondria which stimulates cytochrome c oxidase enzyme resulting in reactive oxygen species (ROS) overproduction. The latter induces an inflammatory condition via increasing production of the nuclear factor kappa-light-chain-enhancer of activated B cells (NF-kB)-dependent inflammatory molecules such as iNOS, TNF-α, IFN-γ, and iL-6 that eventually initiate neurodegenerative and inflammatory changes in the brain[38]. Another mechanism involves increased secretion of adipocytokines, from the adipose tissue, which induces both peripheral and neural inflammation in addition to oxidative damage[35]. The peripheral inflammatory cytokines could also pass through the blood-brain barrier and cause neurons damage[34].

These biochemical findings were confirmed by the histopathological results. H&E-stained sections of HFD group III demonstrated loss of the regular cerebral lamellar

pattern with marked depletion of the cellular elements. This came in line with Wang *et al*.[41] who reported a significant decrement in the neurons' density with the presence of few scattered shrunken neurons. The authors explained that HFD induces direct neuronal damage via disturbance of the CNS fat metabolism and suppression of the membrane proteins' normal function. They also added that HFD decreases BDNF expression resulting in suppression of both synaptic plasticity and cerebral neurogenesis.

Moreover, another histological alteration in HFD group was the infiltration of the neuropil with numerous small dark glial cells, which is referred to as gliosis. This finding was similarly recorded by Xu *et al*.[42], who stated that HFD consumption increases the susceptibility for gliosis in both the cerebrum and cerebellum. Ito *et al*.[43] previously illustrated that microglia are considered resident macrophages, scattered in the brain parenchyma, and become activated as an early response to numerous pathological conditions such as trauma, inflammation, and degeneration.

Congested blood vessels, in HFD-fed rats, were previously observed in the parotid gland[44], the kidneys and lungs[45], the pancreas[46], and the salivary glands[47]. The former researchers explained the congestion as an inflammatory response, induced by the HFD, in order to increase the blood flow to the damaged or fibrotic tissues. They also added that HFD disturbs the homeostasis as well as the capillary walls and induces vascular atherosclerosis, which may ultimately result in hemorrhage. Interstitial hemorrhage was also recorded in between the renal tubules in HFD-fed rats[46]. The hemorrhage could be also attributed to the disrupted tight junctions of the endothelium, and basal lamina under the effect of released matrix metalloproteinases (MMPs) enzymes from the neuroglial cells at the site of neuronal injury[48]. This could also explain the vacuolated neuropil detected in group III. However, Hashem[49] considered the vacuoles in the neuropil as swollen neurons' processes and pre-synaptic nerve endings.

Shrunken neurons with condensed nuclei were detected in group III. Alkan *et al*.[35] detected the same finding and described it as nuclear pyknosis and attributed it to a shortage of cellular energy besides the degradation of the myelin sheath. Also, bizarre, irregularly shaped, darkly stained pyramidal cells surrounded with pericellular halos were detected in group III. Hashem[49] considered these alterations as degenerative changes and attributed the pericellular halos to neurons' shrinkage and processes' withdrawal caused by alterations in the cytoskeleton, which is considered evidence of neurons' death.

Meanwhile, vacuolated endothelial cells and red neurons were also detected in HFD group. Endothelial cells' malfunction in obese rats was earlier explained by the condition of oxidative stress secondary to enhanced nicotinamide adenine dinucleotide phosphate (NADPH) oxidase enzyme activity[50]. The red neurons were described by Kaufmann *et al*.[51] as dying cells within a certain region secondary to neuronal necrotic damage.

Regarding caspase-3 immunostaining, group III exhibited a strong nuclear reaction in many neurons with a subsequent increase of the apoptotic index with respect to the control group. This finding came in line with Suleiman *et al*.[36], who illustrated that obesity suppresses the Bcl-2 expression meanwhile increasing the Bax expression that causes activation of the caspase cascade. The authors added that HFD-induced oxidative stress eventually stimulates apoptosis. Earlier, Alkan and his colleagues[35] also stated that HFD increases the C-Fos expression, that belongs to the immediate early genes family (IEG), that enhances the neuronal death via the activation of certain transcription sites.

GFAP is an intermediate filament, characteristically expressed in the astrocytes. Its increased expression is referred to as astrocytosis, which occurs as a result of astrocytes' activation in response to brain injury, inflammatory condition and/or oxidative stress, in order to fill the tissue defects[52]. In the current work, HFD group III displayed a significant increment in GFAP +ve astrocytes' number together with strong immunoreaction in many astrocytes, which came in agreement with the findings of both Sharma[34] and Bittencourt *et al*.[53] in the brain of HFD-fed rats.

As regards the iNOS immuno-expression, the HFD group III showed a significant elevation in its expression in many neurons, versus the control group. The same finding was reported by Lu *et al*.[54] who recorded iNOS increment in the brains of HFD-fed mice. They clarified that iNOS increment was a neuro-inflammatory response induced by the HFD and mediated by the microglia activation. This finding confirmed the biochemical results of the same group in the current study.

Stevia, a non-caloric natural sweetener, is considered a promising agent in the management of many medical conditions. This is due to its antioxidant, anti-inflammatory, anti-hypertensive and anti-hyperglycemic properties, besides its role in ameliorating insulin resistance and boosting memory[55].

In the present work, concomitant intake of stevia with HFD feeding in group IV significantly reduced the weight gain percentage and the final total body weight. These findings agreed with those recorded by AbdElwahab *et al*.[56] and Faruqi *et al*.[57] who explained them by decreased food intake secondary to stevia consumption, as it regulates both insulin and glucose blood levels. Other explanations include decreased secretion of appetite hormones together with enhanced secretion of anorexic hormones and increased sense of gastric fullness due to the high content of fibers in the stevia extract[58].

Moreover, stevia consumption in group IV caused a significant reduction in TC, TGs and LDLc serum levels together with a significant elevation of HDLc serum level. These results came in accordance with those of Ranjbar

et al.[58] who explained them by various mechanisms. One mechanism involved the enhancement of fat catabolism secondary to enhanced lipoprotein enzyme activity. Another mechanism suggested enhanced oxidation of the fatty acids via elevated hepatic carnitine production. Moreover, similar TC and TGs findings were reported in rats with polycystic ovary (PCO) treated with stevia and were attributed to enhanced hepatic lipase enzyme activity[59].

Stevia co-treated group IV also exhibited a significant increment in CAT, GPx, and SOD together with a significant decrement in MDA and MPO levels. Similarly, Ranjbar *et al*.[58] and El Nashar *et al*.[52] reported an increment in CAT and total antioxidant capacity (TAC) levels as well as a decrement in the MDA level in stevia-treated rats, denoting its antioxidant activity. Morsi *et al*.[59] also recorded a significant increment in SOD and a significant decrement in MDA levels in stevia-treated PCO rats. As regards the decrement in MPO, it could be attributed to stevia's anti-inflammatory properties through suppressing NF-kB inflammatory cascade[52,55].

Meanwhile, the formerly mentioned HFD-induced histopathological findings were ameliorated in the stevia-treated group IV, which were evidenced by the intact compact neuropil with almost no gliosis or vacuolation, more or less normal cortical layers, as well as the preservation of neuronal integrity and appearance. Similar findings were previously recorded in the hippocampus of stevia-treated rats as most of the neuropil appeared almost normal without signs of gliosis[10]. The authors attributed stevia's neuroprotective effect to its antioxidant properties and its elevated polyphenol content compounds and flavonoids. Another recent study, performed by Ali[60], illustrated that stevia extract improved the neuropil appearance and ameliorated the degeneration, vacuolation and apoptosis of the nerve cells in the cerebral cortex of mice treated with nalbuphine. The author attributed these findings to the outstanding ROS scavenging capability and the considerable protective role of stevia versus hydrogen peroxide-induced damage in various tissues.

Moreover, other studies demonstrated similar results in other organs, such as the liver[61] and the testis[62], in which stevia administration ameliorated the histopathological changes caused by HFD-induced type II diabetes.

However, few pyramidal cells were shrunken with dark nuclei and pericellular haloes, along with occasional neuropil vacuoles. Similar nuclear findings were recorded, by Bassit *et al*.[63], in some Purkinje cells in the cerebellar cortex of stevia-treated rats.

In the current work, a significant reduction in the apoptotic index with the presence of moderate reaction in few neurons was also observed in group IV in comparison to group III. This came in line with El Nashar *et al*.[52] who reported a marked reduction in the count of apoptotic nerve cells in the hippocampus of stevia-treated epileptic rats. Stevia was previously recorded to oppose cell death and enhance cell maintenance via suppressing caspase-3 and Bax production while enhancing Bcl2 expression[56]. Similarly, stevia-treated group IV depicted a significant decrement in the GFAP +ve cells' number with moderate immunoreaction in only some cells. This came in agreement with the findings of El Nashar and colleagues[52].

Furthermore, stevia-treated group IV denoted a significant decrement in the iNOS expression versus the HFD group III which was supported by the statistical analysis of the iNOS mean area percentage. This finding was previously observed by Kim *et al*.[64] and Ali[60] who reported that stevia could suppress the secretion of nitric oxide and the pro-inflammatory cytokines. The former illustrated that this effect might be mediated by the suppression of both NF-κB activation and mitogen-activated protein kinase enzyme (MAPK) phosphorylation, which confirms the anti-inflammatory activity of stevia.

CONCLUSION AND RECOMMENDATIONS

Taken together, the results of the current work proved that Stevia Rebaudiana extract greatly protected against HFD-induced cerebral cortex changes. This neuroprotective effect can be attributed to stevia's antioxidant, anti-inflammatory, anti-apoptotic and hypolipidemic actions besides its regulating effect on food intake and weight gain. Thus, this study provided a new insight into a promising future herbal neuroprotective agent. Nevertheless, further pre-clinical and clinical research are mandatory to verify the safety and efficacy of chronic use of Stevia Rebaudiana as a neuroprotective agent.

CONFLICT OF INTERESTS

There are no conflicts of interest.

REFERENCES

1. Elsisy, R. A., El-Magd, M. A., & Abdelkarim, M. A. (2021). High-fructose diet induces earlier and more severe kidney damage than high-fat diet on rats. Egyptian Journal of Histology, 44(2), 535-544. https://dx.doi.org/10.21608/EJH.2020.31508.1304

2. Fki, I., Sayadi, S., Mahmoudi, A., Daoued, I., Marrekchi, R., & Ghorbel, H. (2020). Comparative study on beneficial effects of hydroxytyrosol-and oleuropein-rich olive leaf extracts on high-fat diet-induced lipid metabolism disturbance and liver injury in rats. BioMed Research International, 2020,1315202. https://dx.doi.org/10.1155/2020/1315202

3. Velázquez, K. T., Enos, R. T., Bader, J. E., Sougiannis, A. T., Carson, M. S., Chatzistamou, I., Carson, J. A., Nagarkatti, P. S., & Murphy, E. A. (2019). Prolonged high-fat-diet feeding promotes non-alcoholic fatty liver disease and alters gut microbiota in mice. World journal of hepatology, 11(8), 619. https://doi.org/10.4254/wjh.v11.i8.619

4. Mazzei, G., Ikegami, R., Abolhassani, N., Haruyama, N., Sakumi, K., Saito, T., Saido, T. C. & Nakabeppu, Y. (2021). A high-fat diet exacerbates the Alzheimer's disease pathology in the hippocampus of the App NL− F/NL− F knock-in mouse model. Aging cell, 20(8), e13429. https://doi.org/10.1111/acel.13429

5. Charradi, K., Mahmoudi, M., Bedhiafi, T., Kadri, S., Elkahoui, S., Limam, F., & Aouani, E. (2017). Dietary supplementation of grape seed and skin flour mitigates brain oxidative damage induced by a high-fat diet in rat: Gender dependency. Biomedicine & Pharmacotherapy, 87, 519-526. https://doi.org/10.1016/j.biopha.2017.01.015

6. Mengi, N. (2019). The effects of high cholesterol/high fat diet on endoplasmic reticulum stress and neuronal dysfunction in the hippocampus and cerebral cortex of APOE-/-MICE (Master's thesis, Middle East Technical University). https://hdl.handle.net/11511/43794

7. Wang, J., Zhang, J., Wang, X., & Xu, C. (2021). Short-term high-fat diet promotes increased lysine crotonylation in cerebral cortex. https://doi.org/10.21203/rs.3.rs-878125/v1

8. Peteliuk, V., Rybchuk, L., Bayliak, M., Storey, K. B., & Lushchak, O. (2021). Natural sweetener Stevia rebaudiana: Functionalities, health benefits and potential risks. Experimental and clinical sciences journal, 20, 1412. https://doi.org/10.17179/excli2021-4211

9. Matias, F. B. R., Castro, D. F., & Bernardo, N. O. J. L. C. (2021). Stevia rebaudiana leaf extract reduces blood glucose and visceral fat accumulation in alloxan-induced diabetic mice. Journal of microbiology, biotechnology and food sciences, 10(5), e3347-e3347. https://doi.org/10.15414/jmbfs.3347

10. Mohamed, A. S., El-Shinnawy, N. A., & El-mageid, A. (2019). Difference between natural and artificial sweeteners: Histopathological studies on male albino rat's brain (hippocampus). Journal of Scientific Research in Science, 36(1), 120-139. https://doi.org/10.21608/JSRS.2019.31001

11. Ray, J., Kumar, S., Laor, D., Shereen, N., Nwamaghinna, F., Thomson, A., Perez, J. P., Soni, L., & McFarlane, S. I. (2020). Effects of Stevia rebaudiana on glucose homeostasis, blood pressure and inflammation: a critical review of past and current research evidence. International journal of clinical research & trials, 5. https://doi.org/10.15344/2456-8007/2020/142

12. Kurek, J. M., Król, E., & Krejpcio, Z. (2020). Steviol glycosides supplementation affects lipid metabolism in high-fat fed STZ-induced diabetic rats. Nutrients, 13(1), 112. https://doi.org/10.3390/nu13010112

13. Hussein, A. M., Eid, E. A., Bin-Jaliah, I., Taha, M., & Lashin, L. S. (2020). Exercise and Stevia rebaudiana (R) extracts attenuate diabetic cardiomyopathy in type 2 diabetic rats: possible underlying mechanisms. Endocrine, Metabolic & Immune Disorders-Drug Targets (Formerly Current Drug Targets-Immune, Endocrine & Metabolic Disorders), 20(7), 1117-1132. https://dx.doi.org/10.2174/1871530320666200420084444

14. Keshk, W. A., Ibrahim, M. A., Shalaby, S. M., Zalat, Z. A., & Elseady, W. S. (2020). Redox status, inflammation, necroptosis and inflammasome as indispensable contributors to high fat diet (HFD)-induced neurodegeneration; Effect of N-acetylcysteine (NAC). Archives of biochemistry and biophysics, 680, 108227. https://doi.org/10.1016/j.abb.2019.108227

15. Yeung, D. (2015). Does a high fat diet cause inflammation in female rat brain? (Master's thesis, University of Waterloo). http://hdl.handle.net/10012/9517

16. Sorour, H. A., Salem, M. A., Abdelmaksoud, D. A., Elgalil, A., & Mohamed, M. (2022). The impact of high fat diet and flaxseed on liver histology, histochemistry and morphometry in ovariectomized albino rat. Egyptian Journal of Histology, 45(1), 68-89. https://doi.org/10.21608/EJH.2021.58761.1421

17. Ibrahim, M., Moustafa, K. A. A., & Elkaliny, H. H. (2021). Effect of juvenile obesity on the islets of langerhans in rat and the possibility of recovery at adulthood: A histological and immunohistochemical study. Egyptian Journal of Histology, 44(2), 478-488. https://doi.org/10.21608/EJH.2020.34409.1324

18. Mohammed, N. M., Al-Zubaidy, A. A., Qassim, B. J., Hussein, U. A. R., Alsaesdi, H. F., Mohammed, T. A., Khudur, R. K., & Roomi, A. B. (2021). Neuroprotective and Anti-nociceptive Effects of Roflumilast on Vincristine-Induced Neuropathy in Rats. Annals of the Romanian Society for Cell Biology, 3251-3274. http://annalsofrscb.ro/index.php/journal/article/view/2866

19. Onaolapo, A. Y., Odetunde, I., Akintola, A. S., Ogundeji, M. O., Ajao, A., Obelawo, A. Y., & Onaolapo, O. J. (2019). Dietary composition modulates impact of food-added monosodium glutamate on behavior, metabolic status and cerebral cortical morphology in mice. Biomedicine & Pharmacotherapy, 109, 417-428. https://doi.org/10.1016/j.biopha.2018.10.172

20. Chance, B. M., & Maehly, A. C. (1955). Assay of catalase and peroxidase. Methods in Enzymology, 2(55), 764-775.https://doi.org/10.1016/S0076-6879(55)02300-8

21. Kakkar, P., Das, B., & Viswanathan, P. N. (1984). A modified spectrophotometric assay of superoxide dismutase. Indian journal of biochemistry & biophysics, 21(2), 130-2. http://nopr.niscpr.res.in/handle/123456789/19932

22. Mohandas, J., Marshall, J. J., Duggin, A.H., Horvath, J. S., & Tiller, D. J. (1984). Differential distribution of

glutathione and glutathione-related enzymes in rabbit kidney: possible implications in analgesic nephropathy. Biochemical pharmacology, 33(11), 1801-1807. https://doi.org/10.1016/0006-2952(84)90353-8

23. Ohkawa, H., Ohishi, N., & Yagi, K. (1979). Assay for lipid peroxides in animal tissues by thiobarbituric acid reaction. Analytical biochemistry, 95(2), 351-358. https://doi.org/10.1016/0003-2697(79)90738-3
24. Bradley, P. P., Priebat, D. A., Christensen, R. D., & Rothstein, G. (1982). Measurement of cutaneous inflammation: estimation of neutrophil content with an enzyme marker. Journal of investigative dermatology, 78(3), 206-209. https://doi.org/10.1111/1523-1747.ep12506462
25. Bancroft, J., & Layton, C. (2019). The hematoxylin and eosin, Chapter 10, In: Suvarna S, Layton C and Bancroft J, editors. Bancroft's Theory and Practice of Histological Techniques. 8th ed. Elsevier. China. https://doi.org/10.1016/C2015-0-00143-5
26. Kandeel, S., Abd-Elsalam, M. M., Abd-Elsalam, S., & Elkaliny, H. H. (2024). The possible protective effect of taurine on bisphenol: Induced structural changes on the cerebral cortex of rats: Histological and immunohistochemical study. CNS & Neurological Disorders Drug Targets, 23 (10), 1263-1274. https://doi.org/10.2174/0118715273280701231227100805
27. Shalaby, A. M., Alnasser, S. M., Khairy, D. A., Alabiad, M. A., Alorini, M., Jaber, F. A., & Tawfeek, S. E. (2023). The neuroprotective effect of ginsenoside Rb1 on the cerebral cortex changes induced by aluminium chloride in a mouse model of Alzheimer's disease: A histological, immunohistochemical, and biochemical study. Journal of Chemical Neuroanatomy, 1(129), 102248. https://doi.org/10.1016/j.jchemneu.2023.102248
28. Abdelmoneim, W. M., Bakr, M. H., Ghandour, N. M., Mohammed, M. K., Fawzy, M., Ramadan, A. G., & Abdellah, N. Z. (2023). Cytotoxicity associated with acute and chronic administration of synthetic cannabinoids "Strox" in the brain, liver, heart, and testes of male albino rats: histological and immunohistochemical study. Egyptian Journal of Forensic Sciences, 13(1), 11. https://doi.org/10.1186/s41935-023-00331-8
29. Buchwalow, I. B., & Böcker, W. (2010). Working with Antibodies. In: Immunohistochemistry: Basics and methods, Springer Berlin Heidelberg, 31-39. https://doi.org/10.1007/978-3-642-04609-4_4
30. Abdel-kareem, R., & Domouky, A. (2020). Role of B-carotene against toxic effect of titanium dioxide nanoparticles on cerebral cortex of adult albino rat: Histological and biochemical approach. Egyptian Journal of Histology, 43(2), 441-454. https://doi.org/10.21608/EJH.2019.16387.1160
31. Motawea, S. M., Amer, R. M., Haiba, D. A., & Mostafa, M. S. (2020). Cerebral cortical changes in adult albino rats under the effect of tramadol and its withdrawal: Histological and morphometric study. Egyptian Journal of Histology, 43(2), 412-426. .https://doi.org/10.21608/EJH.2019.14072.1136
32. Dawson, B., & Trapp, R. G. (2004). Basic & Clinical Biostatistics. In: Basic & Clinical Biostatistics. 4th ed. Lange Medical Books / McGraw-Hill Medical Publishing Division, 162-189. https://primo.qatar weill.cornell.edu/permalink/974WCMCIQ_INST/1uk5n69/alma991000014429706691
33. Gzielo, K., Kielbinski, M., Ploszaj, J., Janeczko, K., Gazdzinski, S. P., & Setkowicz, Z. (2017). Long-term consumption of high-fat diet in rats: effects on microglial and astrocytic morphology and neuronal nitric oxide synthase expression. Cellular and molecular neurobiology, 37, 783-789. https://dx.doi.org/10.1007/s10571-016-0417-5
34. Sharma, S. (2021). High fat diet and its effects on cognitive health: alterations of neuronal and vascular components of brain. Physiology & Behavior, 15(240), 113528. https://doi.org/10.1016/j.physbeh.2021.113528
35. Alkan, I., Altunkaynak, B. Z., Gültekin, G. İ., & Bayçu, C. (2021). Hippocampal neural cell loss in high-fat diet-induced obese rats–exploring the protein networks, ultrastructure, biochemical and bioinformatical markers. Journal of Chemical Neuroanatomy, 114, 101947. https://doi.org/10.1016/j.jchemneu.2021.101947
36. Suleiman, J. B., Mohamed, M., Abu Bakar, A. B., Zakaria, Z., Othman, Z. A., & Nna, V. U. (2022). Therapeutic effects of bee bread on obesity-induced testicular-derived oxidative stress, inflammation, and apoptosis in high-fat diet obese rat model. Antioxidants, 11(2), 255.https://doi.org/10.3390/antiox11020255
37. Yousef, S. M. (2022). The potential protective effects of diet fortified with mung bean and soybean against oxidative stress caused by high fat diet in rats. Journal of Research in the fields of Specific Education, 8 (43), 1147-1167. https://doi.org/10.21608/jedu.2022.128609.1626
38. Tan, B. L., & Norhaizan, M. E. (2019). Effect of high-fat diets on oxidative stress, cellular inflammatory response and cognitive function. Nutrients, 11(11), 2579. https://doi.org/10.3390/nu11112579
39. Noeman, S. A., Hamooda, H. E., & Baalash, A. A. (2011). Biochemical study of oxidative stress markers in the liver, kidney and heart of high fat diet induced obesity in rats. Diabetology & metabolic syndrome, 3(17), 1-8. https://doi.org/10.1186/1758-5996-3-17
40. Maciejczyk, M., Żebrowska, E., Zalewska, A., & Chabowski, A. (2018). Redox balance, antioxidant

defense, and oxidative damage in the hypothalamus and cerebral cortex of rats with high fat diet-induced insulin resistance. Oxidative Medicine and Cellular Longevity, 2018.https://doi.org/10.1155/2018/6940515

41. Wang, Z., Fan, J., Wang, J., Li, Y., Xiao, L., Duan, D., & Wang, Q. (2016). Protective effect of lycopene on high-fat diet-induced cognitive impairment in rats. Neuroscience Letters, 627, 185-191.http://dx.doi.org/doi:10.1016/j.neulet.2016.05.014

42. Xu, C. J., Li, M. Q., Chen, W. G., & Wang, J. L. (2021). Short-term high-fat diet favors the appearances of apoptosis and gliosis by activation of ERK1/2/p38MAPK pathways in brain. Aging (Albany NY), 13(19), 23133. https://doi.org/10.18632/aging.203607

43. Ito, D., Tanaka, K., Suzuki, S., Dembo, T., & Fukuuchi, Y. (2001). Enhanced expression of Iba1, ionized calcium-binding adapter molecule 1, after transient focal cerebral ischemia in rat brain. Stroke, 32(5), 1208-1215. https://doi.org/10.1161/01.STR.32.5.1208

44. Selim, S.A. (2013). The effect of high-fat diet-induced obesity on the parotid gland of adult male albino rats: histological and immunohistochemical study. The Egyptian Journal of Histology. 36(4), 772-780. https://doi.org/10.1097/01.EHX.0000437624.80956.78

45. Al-Hayder, M. N., Al-Mayyahi, R. S., Hraishawi, R. M. O. (2020). The effects of high fat diet on kidney and lung histopathology in experimental rats. Open Journal of Science and Technology. 3(1), 40-45. https://doi.org/10.31580/ojst.v3i1.1357

46. Rasheed, R.A., Elshikh, M.S., Mohamed, M.O., Darweesh, M.F., Hussein, D.S., Almutairi, S.M., & Embaby, A.S. (2022). Quercetin mitigates the adverse effects of high fat diet on pancreatic and renal tissues in adult male albino rats. Journal of King Saud University - Science. 34(4), 101946. https://doi.org/10.1016/j.jksus.2022.101946

47. Kandeel, S., & M Elwan, W. (2023). Effect of high fat diet on the rat submandibular salivary glands with the possible protection by Gomisin A: Light and scanning electron microscopic study. Egyptian Journal of Histology, 46(2), 588-602. https://dx.doi.org/10.21608/ejh.2022.100644.1576

48. El-Beltagi, E. M., ElKaliny, H. H., Moustafa, K. A., Soliman, G. M., & Zamzam, A. E. M. F. (2022). Effect of bone marrow-derived mesenchymal stem cells on the hippocampal CA1 area of aluminium chloride-induced alzheimer's disease in adult male albino rat: A histological and immunohistochemical study. Egyptian Journal of Histology, 45(4), 968-985.https://dx.doi.org/10.21608/ejh.2021.78406.1495

49. Hashem, H. (2018). The possible protective role of melatonin on the changes in the cerebral cortex and meninges of streptozotocin-induced diabetes in adult male albino rats (histological and immunohistochemical study). Egyptian Journal of Histology, 41(4), 533-545. https://doi.org/10.21608/ejh.2018.4916.1019

50. White, C. L., Pistell, P. J., Purpera, M. N., Gupta, S., Fernandez-Kim, S. O., Hise, T. L., ... & Bruce-Keller, A. J. (2009). Effects of high fat diet on Morris maze performance, oxidative stress, and inflammation in rats: contributions of maternal diet. Neurobiology of disease, 35(1), 3-13. https://doi.org/10.1016/j.nbd.2009.04.002

51. Kaufmann, W., Bolon, B., Bradley, A., Butt, M., Czasch, S., Garman, R. H., George, C., Groters, S., Krinke, G., Little, P., McKay, J., Narama, I., Rao, D., Shibutani, M., & Sills, R. (2012). Proliferative and non-proliferative lesions of the rat and mouse central and peripheral nervous systems. Toxicologic pathology, 40(4suppl), 87S-157S. https://doi.org/10.1177/0192623312439125

52. El Nashar, E. M., Obydah, W., Alghamdi, M. A., Saad, S., Yehia, A., Maryoud, A., & Hussein, A. M. (2022). Effects of Stevia rebaudiana Bertoni extracts in the rat model of epilepsy induced by pentylenetetrazol: Sirt-1, at the crossroads between inflammation and apoptosis. Journal of Integrative Neuroscience, 21(1), 21. https://doi.org/10.31083/j.jin2101021

53. Bittencourt, A., Brum, P. O., Ribeiro, C. T., Gasparotto, J., Bortolin, R. C., de Vargas, A. R., Heimfarth, L., de Almeida, R. f., Moreira, J. C. F., de Oliveira, J., & Gelain, D. P. (2022). High fat diet-induced obesity causes a reduction in brain tyrosine hydroxylase levels and non-motor features in rats through metabolic dysfunction, neuroinflammation and oxidative stress. Nutritional neuroscience, 25(5), 1026-1040. https://doi.org/10.1080/1028415x.2020.1831261

54. Lu, T., Ding, L., Zheng, X., Li, Y., Wei, W., Liu, W., Tao, J. & Xue, X. (2024). Alisol A exerts neuroprotective effects against HFD-induced pathological brain aging via the SIRT3-NF-κB/MAPK pathway. Molecular neurobiology, 61(2), 753-771. https://doi.org/10.1007/s12035-023-03592-5

55. Khakpai, F., Naseroleslami, M., Moheb-Alian, M., Ghanimati, E., Abdollah-Pour, F., & Mousavi-Niri, N. (2023). Intra-gastrically administration of Stevia and particularly Nano-Stevia reversed the hyperglycemia, anxiety, and memory impairment in streptozotocin-induced diabetic rats. Physiology & Behavior, 263, 114100. https://doi.org/10.1016/j.physbeh.2023.114100

56. AbdElwahab, A. H., Yousuf, A. F., Ramadan, B. K., & Elimam, H. (2017). Comparative effects of Stevia rebaudiana and aspartame on hepato-renal function of diabetic rats: Biochemical and histological approaches. Journal of Applied Pharmaceutical Science, 7(8), 034-042. https://doi.org/10.7324/JAPS.2017.70806

57. Faruqi, A., Subuctageen, S., Mughal, I.A., Parveen, S., Zafar, T., & Irfan, A. (2022). Effect of stevia leaf powder on body weight – An experimental study. Journal of Rawalpindi Medical College, 26(4):637-641. https://www.journalrmc.com/index.php/JRMC/article/view/1993

58. Ranjbar, T., Nekooeian, A. A., Tanideh, N., Koohi-Hosseinabadi, O., Masoumi, S. J., Amanat, S., Azarpira, N., & Monabati, A. (2020). A comparison of the effects of Stevia extract and metformin on metabolic syndrome indices in rats fed with a high-fat, high-sucrose diet. Journal of Food Biochemistry, 44(8), e13242. https://doi.org/10.1111/jfbc.13242

59. Morsi, A.A., Mersal, E.A., Farrag, A.H., Abdelmoneim, A. M., Abdelmonem, A. M., & Salem, M. S. (2022). Histomorphological changes in a rat model of polycystic ovary syndrome and the contribution of stevia leaf extract in modulating the ovarian fibrosis, VEGF, and TGF-β immunoexpressions: comparison with metformin. Acta Histochemica et Cytochemica, 55(1), 9-23. https://doi.org/10.1267/ahc.21-00081

60. Ali, R. (2023). Stevia extract and MK-801 attenuate nalbuphine tolerance and dependence in mice: Role of glutamate, nitric oxide, and oxidative stress. Sphinx Journal of Pharmaceutical and Medical Sciences, 6(1), 1-14. https://doi.org/10.21608/sjpms.2023.233910.1022

61. Emam, R. M., Hussein, A. M., Elmileegy, A. A., El-Menabawy, F. R., & Gad, G. E. A. (2021). Effect of Stevia rebaudiana and exercise on fatty liver in type 2 diabetic rats. Bulletin of Egyptian Society for Physiological Sciences, 41(4), 428-440. https://doi.org/10.21608/besps.2021.48134.1083

62. Elshafey, M., Erfan, O. S., Risha, E., Badawy, A. M., Ebrahim, H. A., El-Sherbiny, M., El-Shenbaby, I., Enan, E. T., Almadani, M. E., & Eldesoqui, M. (2023). Protective effect of Stevia on diabetic induced testicular damage: an immunohistochemical and ultrastructural study. European Review for Medical and Pharmacological Sciences, 27(22), 11039-11056. https://doi.org/10.26355/eurrev_202311_34473

63. Bassit, A. S., Esmail, Z. M., Abdelall, A. H., Khalaf, A. M., & Ali, H. (2021). Comparative study between the effect of aspartame and stevia on the Purkinje cells of the cerebellar cortex of albino rats. (electron microscopic study). Sohag Medical Journal, 25(2), 93-99. https://doi.org/10.21608/smj.2021.72094.1244

64. Kim, S. Y., Jo, M. J., Hwangbo, M., Back, Y. D., Jeong, T. Y., Cho, I. J., & Jee, S. Y. (2013). Anti-inflammatory effect of Stevia Rebaudiana as a results of NF-κB and MAPK inhibition. The Journal of Korean Medicine Ophthalmology and Otolaryngology and Dermatology, 26(3), 54-64. https://doi.org/10.6114/jkood.2013.26.3.054

الملخص العربى

دراسة هستولوجية وهستوكيميائية مناعية لتأثير مستخلص ستيفيا ريبوديانا على القشرة المخية لذكر الجرذ الأبيض البالغ المغذى بنظام غذائي عالي الدهون

منى تيسير صادق[١]، مروة عوض عبد الحميد إبراهيم[١]، دعاء أحمد رضوان[٢]، دينا فؤاد الشاعر[١]

[١]قسم علم الأنسجة وبيولوجيا الخلية، [٢]قسم التشريح الأدمي وعلم الأجنة، كلية الطب، جامعة طنطا، مصر

المقدمة: تعد السمنة تحدى صحى عالمى متعلق بالعديد من الإضطرابات المعرفية والتنكسية العصبية. ويعد النظام الغذائى عالى الدهون هو السبب الرئيسى للسمنة فى الإنسان والطريقة المعتمدة لإحداثها فى حيوانات التجارب. بينما يعتبر ستيفيا ريبوديانا - وهو مُحلي طبيعي خالي من السعرات الحرارية - عنصراً واعداً في التعامل مع العديد من الحالات الطبية نظراً لتأثيراته المضادة للأكسدة، والمضادة لموت الخلايا المبرمج، والمضادة للإلتهابات، وكذلك الخافضة لشحميات الدم.

الهدف من الدراسة: لتقييم تأثير مستخلص ستيفيا ريبوديانا على القشرة المخية لذكر الجرذ الأبيض البالغ المغذى بنظام غذائي عالي الدهون.

المواد وطرق البحث: تم توزيع أربعين جرذ بشكل عشوائي إلى أربع مجموعات متساوية؛ مجموعة ضابطة، مجموعة استيفيا التي غذيت بنظام غذائي متوازن وتلقت مستخلص ستيفيا ريبوديانا بجرعة ٤٠٠ مجم / كجم / يوم عن طريق الفم لمدة ١٠ أسابيع متتابعه، مجموعة النظام الغذائي عالي الدهون التي غذيت يوميًا بنظام غذائي عالي الدهون لمدة ١٠ أسابيع متتابعه ، ومجموعة النظام الغذائي عالي الدهون مع استيفيا التي غذيت يوميًا بنظام غذائي عالي الدهون بالتزامن مع مستخلص ستيفيا ريبوديانا بنفس الجرعة والطريقة مثل المجموعة الثانية لمدة ١٠ أسابيع متتابعه .ومن ثم تم تجهيز عينات القشرة المخية للدراسات الكيميائية الحيوية والهستولوجية والهستوكيميائية المناعية.

النتائج: أظهرت مجموعة النظام الغذائي عالي الدهون ارتفاع ذو دلالة احصائية في أوزان الجسم النهائية وفي نسبة زيادة الوزن ،وكذلك في مستويات TCو TGs و LDLc في المصل ومستويات MDA و MPO في الأنسجة كما أظهرت انخفاض ذو دلالة احصائية في مستوى HDL في المصل ومستويات CAT و GPx وSOD في الأنسجة. علاوة على ذلك، أظهرت مجموعة النظام الغذائي عالي الدهون تغيرات نسيجية ملحوظة في القشرة المخية وارتفاع ذو دلالة احصائية في التعبيرالهستوكيميائي المناعي لـ caspase-٣ وGFAP وiNOS. وقد وجد أن إعطاء مستخلص ستيفيا ريبوديانا بالتزامن مع النظام الغذائي عالي الدهون قد منع معظم هذه التغيرات الكيميائية الحيوية والهستولوجية والهستوكيميائية المناعية.

الإستنتاج: النتائج التي تم الحصول عليها سلطت الضوء على أن مستخلص ستيفيا ريبوديانا كان له تأثير تحسيني قوي ضد التأثيرات الضارة الناجمة عن النظام الغذائي عالي الدهون على القشرة المخية للجرذان.